Foxp1 regulates neural stem cell self-renewal and bias toward deep layer cortical fates

Caroline Alayne Pearson[1,2,3], **Destaye M. Moore**[1,2,3], **Haley O. Tucker**[4], **Joseph D. Dekker**[4], **Hui Hu**[5], **Amaya Miquelajáuregui**[6], **Bennett G. Novitch**[1,2,3,7,*]

[1]Department of Neurobiology, David Geffen School of Medicine at UCLA, Los Angeles, CA 90095, USA

[2]Eli and Edythe Broad Center of Regenerative Medicine and Stem Cell Research, Los Angeles, CA 90095, USA

[3]Intellectual and Developmental Disabilities Research Center, David Geffen School of Medicine at UCLA, Los Angeles, CA 90095, USA

[4]Molecular Biosciences, University of Texas at Austin, Austin, Texas 78712

[5]Department of Microbiology, School of Medicine, University of Alabama at Birmingham, Birmingham, AL 35205

[6]Institute of Neurobiology, University of Puerto Rico Medical Sciences Campus, San Juan 00911, Puerto Rico

[7]Lead Contact

SUMMARY

The laminar architecture of the mammalian neocortex depends on the orderly generation of distinct neuronal subtypes by apical radial glia (aRG) during embryogenesis. Here, we identify critical roles for the autism risk gene *Foxp1* maintaining aRG identity and gating the temporal competency for deep layer neurogenesis. Early in development, aRG express high levels of Foxp1 mRNA and protein, which promote self-renewing cell divisions and deep layer neuron production. Foxp1 levels subsequently decline during the transition to superficial layer neurogenesis. Sustained Foxp1 expression impedes this transition, preserving a population of cells with aRG identity throughout development and extending the early neurogenic period into postnatal life. FOXP1 expression is further associated with the initial formation and expansion of basal RG (bRG) during human corticogenesis and can promote the formation of cells exhibiting characteristics of bRG when misexpressed in the mouse cortex. Together, these findings reveal broad functions for Foxp1 in cortical neurogenesis.

*Correspondence: bnovitch@ucla.edu.

DECLARATION OF INTERESTS

The authors declare no competing interests.

eTOC BLURB

Neocortical progenitors generate distinct cell types in a temporal sequence, yet the mechanisms controlling this process are unclear. Pearson et al. show that the autism risk gene Foxp1 contributes by maintaining apical radial glia character and promoting deep layer neurogenesis. The association of FOXP1 with human corticogenesis is also investigated.

INTRODUCTION

The development of the central nervous system (CNS) depends on a pool of self-renewing neural stem cells (NSCs) being maintained over a protracted period of time to ensure the appropriate numbers of neurons and glia are generated. In the developing neocortex, neuroepithelial progenitors transition into apical radial glia (aRG), which possess the ability to self-renew, directly generate neurons, or give rise to basal secondary progenitors (BPs), most notably intermediate progenitors (IP) and basal radial glia (bRG) (Taverna et al., 2014). BP generation results in the formation of two proliferative zones: the ventricular zone (VZ) composed of aRG and the adjacent subventricular zone (SVZ) where BPs reside (Taverna et al., 2014). The increased size and complexity of the neocortex in higher mammals is attributed to enlargement of the SVZ resulting from expanded bRG formation (Lui et al., 2011; Florio and Huttner, 2014). Disruptions in neural progenitor maintenance and the balance between proliferative growth and differentiation are thought to underlie many neurodevelopmental disorders (Bae et al., 2015; Ernst, 2016); however, the genetic and cellular mechanisms governing these processes are not well understood.

The laminar organization of the mature neocortex is established during embryogenesis by the sequential generation of early-born deep layer (DL) neurons followed by later-born superficial layer (SL) neurons (Okano and Temple, 2009; Greig et al., 2013). A long-standing question has been how aRG produce specific types of neurons at appropriate times in development. Both viral and recombination-based lineage tracing studies have demonstrated that aRG present at the onset of neurogenesis have the capacity to give rise to all cortical neuron types (Gao et al., 2014; Ma et al., 2018). As neurogenesis proceeds, aRG lose their potential to give rise to DL neurons and begin to generate SL neurons (Kwan et al., 2012; Greig et al., 2013; Dwyer et al., 2016). While this "temporal competency" model is appealing, it remains unclear how early aRG are biased to form DL neurons and how they change their neurogenic output. Indeed, a contrasting model whereby DL vs. SL neurons are produced by distinct progenitors rather than through temporal switching of a common pool has been proposed (Franco and Muller, 2013).

Foxp proteins are a family of transcriptional repressors vital for the development of blood, lungs, heart, and the CNS (Wang et al., 2004; Hu et al., 2006; Shu et al., 2007; Dasen et al., 2008; Rousso et al., 2008; Rousso et al., 2012; Wang et al., 2014). Foxp1/2/4 are notably expressed throughout the developing cortex in both dividing progenitors and differentiated cell types (Ferland et al., 2003; Hisaoka et al., 2010; Araujo et al., 2015), and mutations, particularly in *Foxp1*, have been linked to a range of cognitive defects in humans including autism spectrum disorders (ASD) (Lai et al., 2001; Groszer et al., 2008; Hamdan et al., 2010; Horn et al., 2010; O'Roak et al., 2011; Le Fevre et al., 2013; Bacon et al., 2015;

Sanders et al., 2015; Meerschaut et al., 2017). Previously, we have shown that Foxp4 promotes the differentiation of progenitors in both the spinal cord and cortex by repressing the expression of N-Cadherin, a central component of adherens junctions which are critical for NSC maintenance (Rousso et al., 2012). The function of other Foxp proteins in neural progenitors, however, remains unclear.

In this study, we demonstrate that Foxp1 function influences the maintenance of early aRG identity and the timing of neurogenic waves in the developing neocortex. Foxp1 is expressed at the outset of cortical neurogenesis and progressively declines as cells transition from DL to SL neuron production. Gain or loss of Foxp1 function alters the symmetry of aRG divisions and the decision to self-renewal or differentiate. Maintenance or acute misexpression of Foxp1 promotes the formation of DL neurons at the expense of SL neurons and glia. Additionally, sustained Foxp1 expression can extend the formation of early born cell types into postnatal stages. We lastly show that FOXP1 is similarly expressed by aRG cells in the developing human cortex, but in contrast to mouse, is also associated with bRG. Acute elevation of FOXP1 during the peak neurogenic period in the mouse cortex promotes maintenance of Pax6 expression in basal cells that exhibit bRG-like features, suggesting that FOXP1's ability to promote RG identity may be further utilized to generate and expand bRG in the human brain.

RESULTS

Foxp1 is expressed by aRG and downregulated during the transition from early to late neurogenesis

To assess the role of Foxp1 in cortical neurogenesis, we analyzed its expression in mouse cortex from embryonic days (E) 9.5 to 16.5. *Foxp1* mRNA expression is dynamic in the VZ, steadily increasing in expression from E10.5-E12.5 followed by a marked decline between E13.5-E16.5 (Figures 1A-1I). By contrast, *Foxp1* in the cortical plate (CP) remained steady. Nearly identical results were seen with Foxp1 antibody staining (Figures 1J-1R). Over the same time period, staining for other VZ-associated transcription factors such as Sox2 remained constant (Figures S1A-S1D). The expression of Foxp1 within VZ progenitors notably concurs within the temporal window of DL neurogenesis from E10.5-E13.5, marked by the initial appearance of Tbr2 IP in the SVZ followed by Tbr1$^+$ and Ctip2$^+$ DL neurons in the CP, many of which retained Foxp1 expression (Figures 1K-1N, 1S). The observed decline in Foxp1 expression starting around E13.5 coincides with the period of mid-late neurogenesis associated with the production of Lhx2$^+$ SL neurons (Figures 1S and 1T).

Within the VZ, Foxp1 expression was coincident with the aRG-associated protein Pax6, with > 90% of the Foxp1$^+$ cells expressing both markers at E11.5-E12.5 (Figures 1U-1W, 1CC). The remainder of the Foxp1$^+$ cells expressed the IP marker Tbr2 (Figures 1X-1Z, 1CC), reflecting their progression towards neurogenic differentiation. Analysis of bRG cells outside of the VZ (Pax6$^+$/phosphorylated Vimentin$^+$ cells) at E14.5 and E16.5 showed no evidence of Foxp1 expression in bRG (n = 23 bRG in 13 E14.5 embryos; n = 27 bRG in 6 E16.5 embryos; Figures 1AA and 1BB). Collectively, these data show that Foxp1 expression is selectively expressed by early aRG during DL neurogenesis, and progressively

downregulated from these cells as they transition to SL production and gliogenesis (Figure 1DD).

Foxp1 promotes aRG maintenance

To determine the role of Foxp1 in early aRG, we conditionally elevated or ablated Foxp1 expression by crossing mice carrying $Emx1^{Cre}$ alleles which drive recombination in NSCs starting at E10 (Gorski et al., 2002; Iwasato et al., 2004), to those harboring either a Cre-inducible transgene driving Foxp1 expression from the CAG enhancer/promoter ("Foxp1^{ON}" condition; Wang et al., 2014) or a Cre-inactivatable Foxp1 allele ("Foxp1^{OFF}" condition; Feng et al., 2010) (Figures S2A and S2B). $Emx1^{Cre}$-negative littermate controls were used in all experiments. Recombination, revealed by GFP expression in Foxp1^{ON} embryos or a td-Tomato reporter cassette bred into the Foxp1^{OFF} background, initially occurs in the ventrolateral and medial cortex (Figures S2C and S2F). By E11.5, recombination occurs dorsally in the lateral cortex extending to the entire lateral cortex by E12.5 (Figures S2D-S2E and S2G-S2H). In Foxp1^{ON} embryos, the coincidence of GFP and elevated Foxp1 expression strongly overlaps (Figure S2C-S2E and S2I-S2K). Ablation of Foxp1 appears to be slightly delayed in Foxp1^{OFF} cortices (Figures S2F, S2G, S2L and S2M). By E12.5, no Foxp1 is detected in the cortex (Figures S2L-S2Q). The Foxp1^{ON} transgene used in these experiments appeared to increase protein expression 3-fold compared to unrecombined E13.5-E14.5 controls, rising to 12-fold at E16.5, as Foxp1 is detectable at very low levels at this time. Nevertheless, the overall level of Foxp1 expression in Foxp1^{ON} cortices did not exceed physiological levels seen in other brain regions such as the lateral ganglionic eminences (Figure S2R-S2T). Foxp1 manipulation also did not appear to affect expression of either Foxp2 or Foxp4 (Figures S2U-S2X).

Next, we examined the effects of Foxp1 manipulation on cortical progenitors (aRG, IPs and bRG). In E13.5 Foxp1^{ON} cortices, Pax6$^+$ aRG increased in number while Tbr2$^+$ IP declined (Figures 2A-2B, 2D-2F). Conversely, in Foxp1^{OFF} cortices a decrease in aRG and increase in SVZ IP was observed (Figures 2A, 2C-2E, 2G). On average, we observed a 2.5:1 ratio of Pax6$^+$ aRG to Tbr2$^+$ IP in control cortices. This ratio increased to 3.4:1 in Foxp1^{ON} cortices and decreased to less than 2:1 in Foxp1^{OFF} embryos (Figure 2H). This phenotype was preserved at both mid and late stages of neurogenesis in Foxp1^{ON} cortices, (Figures 2I-2L). However, there were no significant differences in aRG or IP number in the Foxp1^{OFF} cortices at these time points (Figures 2I-2K, 2M). At E14.5 we also observed an increase in the number of Pax6$^+$ Tbr2$^-$ bRG in both Foxp1^{ON} and Foxp1^{OFF} cortices (Figures 2K-2N). This boost in bRG was transient in Foxp1^{OFF} cortices, as no such increase was seen at E16.5 but appeared to be sustained under Foxp1^{ON} conditions (Figure 2N).

We lastly examined the impact of Foxp1 manipulation on progenitor proliferation through Bromodeoxyuridine (BrdU) labeling of cells in S-phase and quantification of mitotic cells using phosphorylated Histone H3 (pH3) immunostaining. In Foxp1^{ON} embryos, there was a significant increase in the number of BrdU$^+$ cells in the VZ, though no clear change in Foxp1^{OFF} specimens (Figures 2O-2Q, 2U). However, the distribution of BrdU$^+$ cells within the SVZ appeared to be altered under both conditions. In Foxp1^{ON} embryos there was a 48.9% reduction in the percentage of BrdU$^+$ cells in the SVZ, whereas in Foxp1^{OFF} embryos

where was a 42% increase (Figures 2O-2Q, 2V). These changes in BrdU incorporation coincided with differences in pH3 staining, with Foxp1[ON] cortices showing increases in the number of apical and basal mitotic cells, and Foxp1[OFF] cortices showing reductions in apical mitoses alone (Figures 2R-2T, 2W). Together, these data demonstrate that Foxp1 manipulation affects the proliferative activity of aRG, with Foxp1 activation favoring aRG self-renewal and maintenance, and Foxp1 loss having the opposite effect.

Foxp1 promotes vertical, symmetric self-renewing cell divisions

NSC self-renewal, where at least one cell maintains an aRG identity, are commonly associated with vertical cell divisions, defined as cells exhibiting a rotational angle of 60 —90° relative to the apical (ventricular) plane. Early in development, most aRG undergo aRG-aRG vertical divisions to expand the progenitor pool. During mid-neurogenic phases, neural progenitors continue to undergo vertical divisions, but with an increased incidence of aRG-IP or aRG-neuron ($-$N) outcomes. A subpopulation of aRG also undergo non-vertical divisions (0-60°) that are not self-renewing, giving rise to IPs and neurons (Konno et al., 2008; Lancaster and Knoblich, 2012). In E13.5 control cortices, the majority of aRG divisions were vertical (mean angle $65.5 \pm 1.6°$ SEM) with a minority fraction appearing non-vertical, reflecting the propensity of the progenitors to undergo self-renewing divisions at this developmental stage (Figure 3B). In Foxp1[ON] mice, mitoses were even more biased towards vertical divisions with a mean division angle of $73 \pm 1.4°$ SEM and a 1.4-fold increase in the overall incidence of vertical divisions (Figures 3B-3C). Foxp1[OFF] cortices displayed the opposite trend, with a reduction in the mean angle of divisions to $61.2 \pm 2.5°$ SEM and > 2-fold increase in the frequency of non-vertical mitoses (Figures 3B-3C). Thus, Foxp1 appears to promote vertical aRG divisions, which are a characteristic feature of early aRG.

To further analyze the mode of progenitor cell divisions, we performed paired cell assays in which cells are dissociated from E13.5 control, Foxp1[ON], and Foxp1[OFF] cortices, plated at clonal density, and cultured for 20 hours (Figures 3D-3E). We then located couplets of cells (the result of single progenitor divisions) and determined their identities using Pax6, Tbr2 and TUJ1 immunostaining to respectively distinguish aRG, IP, and neurons (Figures 3E-3F). Couplets were accordingly categorized as RG-RG, RG-IP, RG-N, IP-IP, and IP-N (Figure 3G-3H). In this assay, RG isolated from control cortices predominantly displayed asymmetric RG-IP divisions rather than symmetric RG-RG divisions, at an approximately 2.1:1 ratio (Figures 3I-3J). By contrast, RG isolated from Foxp1[ON] cortices displayed significantly more RG-RG and fewer RG-IP cell divisions such that their relative ratio was 1:1.3 (Figures 3I-3J). Foxp1 loss did not appear to alter the fate decisions of RG couplets compared to control cortices (Figures 3I-3J), possibly reflecting the endogenous downregulation of Foxp1 in controls by this time point such that they become indistinguishable from the Foxp1[OFF] samples. Together, these analyses demonstrate that Foxp1 promotes symmetric, population-expanding vertical aRG divisions, impacting both the size of the aRG compartment and formation of IP cells in vivo.

Foxp1 maintenance promotes the generation of early born neurons

Given its effects on aRG behavior, we next asked how Foxp1 manipulation affects cortical neurogenesis. At E13.5, Foxp1^{ON} cortices showed deficits in the formation of early born cell types including Tbr1^{+} DL neurons and Calretinin^{+} layer I neurons, while an increase in both cell types was detected in Foxp1^{OFF} cortices (Figures 4A-4C, 4M, S3A-S3D). At later stages of embryogenesis (E18.5), a significant decrease in the number of cells expressing the pan neuronal marker Myt1l was observed in Foxp1^{OFF} embryos (Figures 4D-4F, 4N). These analyses together suggest that sustained Foxp1 expression promotes aRG maintenance at the expense of neuronal differentiation, whereas Foxp1 deletion foreshortens the early period of corticogenesis leading to neuronal deficits by late embryogenesis. Cell death, evidenced by cleaved Caspase3 staining, did not appear to be grossly impacted by either Foxp1 manipulation (Figures S3E-S3I).

To examine how Foxp1 misexpression or deletion from progenitors impacts the establishment of different cortical neurons, we analyzed the number of DL neurons (Tbr1^{+}, Ctip2^{+}) and SL neurons (Cux1^{+}) throughout the CP at E18.5. All measurements were taken from the lateral cortex (motor and somatosensory regions). In Foxp1^{ON} embryos, we found that the number of Tbr1^{+} or Ctip2^{+} DL neurons was significantly increased (Figures 4G, 4H, 4O). By contrast, SL Cux1^{+} neurons were reduced (Figures 4J, 4K, 4O). Conversely, Foxp1 loss resulted in deficits in both Ctip2^{+} and Tbr1^{+} neurons (Figures 4G, 4I, 4O), though the number of late born Cux1^{+} neurons was not affected (Figures 4J, 4L, 4O).

To confirm that the observed changes in DL vs. SL neurogenesis were consequences of upregulating Foxp1 in progenitors rather than neurons, we compared our findings based on *Emx1^{Cre}*-mediated activation to those achieved using *Nex1^{Cre}* mice, where Cre-mediated recombination is restricted to neurons (Goebbels et al., 2006; Figures S4A-S4H). In *Nex1^{Cre}*; Foxp1^{ON} cortices, no changes in the formation of DL Tbr1^{+} or Ctip2^{+} neurons or Cux1^{+} SL neurons were observed (Figures S4I-S4O). Thus, the influence of Foxp1 manipulation on neuronal fate specification appears due to its actions in aRG rather than neurons.

We also asked whether Foxp1 manipulation impacted gliogenesis by costaining for Brain lipid-binding protein (BLBP) and Sox2 to identify immature astrocytes in E18.5 embryos. Only BLBP^{+} Sox2^{+} cells outside of the VZ/SVZ were counted to distinguish these cells from aRG which also express these markers (Figure S4S). Foxp1^{ON} embryos showed reductions in BLBP^{+} Sox2^{+} cells, while there were no changes in Foxp1^{OFF} embryos (Figures S4P-S4T). Together, these data demonstrate that elevated/sustained levels of Foxp1 in aRG promote the generation of early born neurons at the expense of later born neurons and glia. Foxp1 loss on the other hand leads to selective deficits in early but not late-born neurons and glia, reflecting the early role of Foxp1 in aRG prior to its downregulation during mid neurogenesis.

Sustained Foxp1 expression extends the temporal window of early neurogenesis

The association of Foxp1 function with DL neurogenesis lead us to ask whether Foxp1 misexpression could extend the duration of DL neurogenesis. We accordingly electroporated

cells within the lateral cortex with either control nEGFP or Foxp1-IRES-nEGFP expression constructs at E13.5 and analyzed the spatial distribution and molecular identities of GFP^{+} cells at P0.5 using Tbr1 and Ctip2 to distinguish DL neurons, and Lhx2 for SL neurons (Figures 4P-U). After electroporation with the control vector, GFP^{+} cells were predominantly localized in the SL (demarcated by condensed Lhx2^{+} cells), with >70% of GFP^{+} cells expressing Lhx2 (Figures 4T, 4W). By contrast, cells transfected with Foxp1-IRES-nEGFP plasmids were distributed throughout the CP, and frequently expressed Tbr1 and Ctip2 rather than Lhx2 (Figures 4Q, 4S, 4U, 4W). A subset of the Foxp1-transfected cells was also found in layer I and expressed Calretinin, a result that was not observed with the nEGFP control vector (arrowheads in Figures 5B, 5D, S5A-S5B). We also observed ectopic clusters of GFP[+]/Tbr1^{+} and GFP[+]/Ctip2^{+} neurons resembling heterotopias in Foxp1-electroporated cortices but not in control pups (Figures S5C-S5G, controls in Figures 4P, 4R, 4T).

To further characterize Foxp1's capacity to prolong the generation of DL neurons, we performed neuronal birthdating analysis by injecting pregnant Foxp1[ON] dams with BrdU at E12.5, E14.5 or E16.5 and collecting embryos at E18.5 (Figure S6A). We then analyzed the association of the BrdU label with expression of markers associated with DL or SL neurons (Figure S6B). Given the endogenous downregulation of Foxp1 and no apparent change to the later stages of neurogenesis in Foxp1[OFF] embryos, we restricted our analysis to Foxp1[ON] animals. In control cortices, BrdU injections at E12.5 labeled approximately 60% of Tbr1^{+} neurons (within Layer VI) born during or after that time point (Figures S6C, S6O). BrdU labeling of Tbr1^{+} neurons diminished with E14.5 injections and was rare at E16.5 (Figures S6G, S6K, S6O). Lhx2^{+} neurons (within the SL) by contrast were readily labeled by BrdU injections at either E12.5 or E14.5 with a decline seen only at E16.5, reflecting the end of neurogenesis (Figures S6E, S6I, S6M, S6P). Foxp1[ON] embryos displayed a marked increase in number of Tbr1^{+} neurons labeled by BrdU injections at E14.5 or E16.5 (Figures S6H, S6L, S6P). Conversely, the percentage of Lhx2^{+} late born neurons labeled by BrdU administration at E12.5 or E14.5 was reduced (Figures S6J, S6N, S6P). BLBP[+] astrocyte progenitors marked by BrdU labeling at E16.5 was similarly suppressed (Figures S6Y-S6AA).

We next asked whether Foxp1 maintenance could prolong DL neurogenesis into postnatal life by administering BrdU to pregnant dams at E18.5 and collecting cortices at P1.5 (Figure S6U). Analysis of BrdU[+]/Myt1l^{+} neurons throughout the lateral cortex revealed that a small number of neurons are born during this period in control pups (average 5.7 ± 0.9 cells per section, Figures S6Q, S6W). This number increased to an average of 10 ± 1.2 cells per section in Foxp1[ON] pups, along with an overall increase in the percentage of BrdU^{+} cells that were Myt1l^{+} (Figures S6R, S6V, S6W). Analysis of BrdU^{+} cells within the DL further revealed a >2-fold increase in both total numbers and percentage of BrdU[+] Tbr1^{+} cells in Foxp1[ON] pups (Figures S6S-S6T, S6V, S6X). Collectively, these data demonstrate that sustained Foxp1 expression can extend the period of DL neurogenesis into late embryogenesis and postnatal life, while impeding the formation of later born cells including SL neurons and astroglia.

Foxp1 can sustain an aRG-like population into adulthood

Given the ability of Foxp1 to promote aRG maintenance, we asked whether sustained expression of Foxp1 into adulthood could alter the transformation of these progenitors into adult NSCs. Emx1^{Cre}-mediated recombination occurs within the dorsal SVZ adjacent to the lateral ventricles (LV) (Young et al., 2007), a major site of adult neurogenesis. At early postnatal stages, aRG are depleted as they give rise to astrocytes, ependymal cells, and adult NSC of the SVZ (commonly referred to as B1 cells) (Lim and Alvarez-Buylla, 2016). Initial analyses of the gross morphology of adult brains from Foxp1^{ON} animals compared to littermate controls demonstrated no overt differences in cortical size or morphology. However, analysis of sections revealed a significant increase in the area of the LV in Foxp1^{ON} forebrains (Figures 5A-5C).

B1 cells typically express Sox2 along with low levels of Pax6, have cell bodies located away from the edge of the ventricle, and extend thin GFAP$^+$ protrusions towards the LV between ependymal cells (Figures 5D, 5F, 5H, 5J). By comparison, aRG have high levels of Sox2 and Pax6, tight somatic packing along the ventricle, and prominent perinuclear GFAP staining (Figure S7A). In 6-week-old Foxp1^{ON} mice, GFAP$^+$ cells lining the dorsal LV appeared more similar to embryonic aRG than B1 cells (Figures 5F-5G, Figures S7B; perinuclear GFAP staining quantified in 5T). The number of Pax6$^+$ cells lining the LV significantly increased, from 32% of DAPI$^+$ cells in controls to 80% in Foxp1^{ON} animals (Figures 5H-5I, 5U), and appeared to form a stratified neuroepithelium distinct from that seen in controls (Figures 5E, 5K). Foxp1^{ON} animals further showed an increased number of Foxj1$^+$ cells lining the LV, the majority of which misexpressed Pax6$^+$ (Figures 5N-6O, 5W). Two recent studies have demonstrated that FoxJ1$^+$ ependymal cells and B1 cells are derived from embryonic aRG (Ortiz-Alvarez et al., 2019; Redmond et al., 2019). The presence of Pax6$^+$/Sox2$^+$/FoxJ1$^+$ cells thus suggests either the persistence of cells with embryonic aRG character or the maintenance of an uncommitted progenitor population. Despite these changes, the ependymal lining of the LV, distinguished by S100 staining, was nevertheless preserved (Figures 5P-5Q).

Type B1 cells generate transit amplifying neuronal precursors (type C cells, Ascl1$^+$) which in turn produce neuroblasts (type A cells, Dcx$^+$) and postmitotic neurons (Lim and Alvarez-Buylla, 2016). Type C cells were slightly reduced in Foxp1^{ON} animals (Figures 5R-5S, 5X), whereas we found a 2-fold increase in the number of Dcx$^+$ cells (Figures 5L-5M, 5 V). While Dcx is frequently used as a marker of type A cells, it is also highly expressed by newborn neurons formed by embryonic aRG. We surmise that the increased numbers of Dcx$^+$ cells seen here may thus reflect this mode of production. Collectively, these data show that Foxp1 misexpression can alter the course of postnatal neurogenesis by maintaining a population of cells with aRG-like properties throughout embryogenesis and into adult life.

Foxp1 is expressed by aRG and bRG in the developing human cortex

In light of the association of *FOXP1* mutations with neurodevelopmental defects, we investigated whether FOXP1 was similarly associated with aRG in the human cortex. FOXP1 was expressed throughout the VZ from GW13-15 (the approximate equivalent to E12.5-E14.5 in mouse), with nearly all cells expressing aRG markers such as SOX2 and

PAX6, and a smaller population (<10%) expressing TBR2 (Figures 6A-6F, 6K). Starting at GW14, FOXP1 also became detectable in many cells scattered throughout the inner and outer subventricular zones (iSVZ and oSVZ; Figures 6A-6E, arrowheads). The bRG identity of these FOXP1$^+$ cells was confirmed by costaining with canonical bRG markers including SOX2, PAX6 and HOPX (Figures 6C, 6E, 6F). At GW14 ~70% of bRG express FOXP1 and ~50% at GW15 (Figure 6L). We further detected FOXP1 in mitotic bRG (pVIM$^+$/PAX6$^+$; Figures 6G-6J), a result that contrasts with the lack of overlap seen in mice (Figures 1 AA, 1BB).

FOXP1 levels progressively declined in both aRG and bRG between GW15-17 (equivalent to E14.5-E16.5 in mouse), coinciding with the transition from mid to late neurogenesis in the human cortex (Nowakowski et al., 2016). At GW17, low levels of FOXP1 were present in bRG (Figures S8A-S8E). However, FOXP1 expression in both aRG and bRG was extinguished by GW21, coinciding with the start of gliogenesis (equivalent to E16.5 onwards in mouse; Figures 6P, 6T). Thus, as with mice, high FOXP1 levels in aRG demarcate the early period of neurogenesis in human cortical development, whereas lower levels are associated with late neurogenesis. In addition, high levels of FOXP1 are also associated with the stages at which bRG are first formed and the oSVZ begins to markedly expand (Figure 6U).

Acute misexpression of human and mouse Foxp1 preserves progenitor characteristics

Given that early manipulation of Foxp1 can impact progenitor identities, and the similarities between mouse and human Foxp1 expression, we examined whether its activity might alter cell fates at the time at which endogenous levels of Foxp1 are declining. To distinguish the early effects of Foxp1 on progenitor maintenance seen in our transgenic Foxp1^{ON} mice from later effects, we used *in utero* electroporation to deliver mouse Foxp1-IRES-nEGFP, human FOXP1-IRES-nEGFP, or nEGFP-only control expression plasmids into wild type mouse lateral cortices at E13.5.

At 2 days post electroporation (dpe; E15.5), misexpression of either mouse (m) or human (h) Foxp1 more than doubled the fraction of GFP$^+$ cells retained within the VZ compared to GFP-only controls and reduced the number of GFP$^+$ cells in the CP (Figures 7A-7C, 7H). Additionally, both Foxp1 constructs led to ectopic expression of Pax6 throughout the IZ with ~85% of the GFP$^+$ cells containing Pax6 after mFoxp1 electroporation and >95% following hFOXP1 transfection (Figures 7D-7G). Some GFP$^+$ cells in the IZ also expressed neuronal markers such as Myt1l, indicating that at least some of the ectopic Pax6$^+$ cells are capable of undergoing neural differentiation (Figures S9A-S9C).

In a third of embryos electroporated with hFOXP1, GFP$^+$ neural rosette structures were detected in the lateral cortex 2 dpe (Figures 7I-7K). These rosettes exhibited apicobasal polarity characterized by apical aPKC staining and formation of small ventricle-like spaces with pH3$^+$ cells undergoing mitosis along the edge. Moreover, Tbr2$^+$ IP were found around the circumference of the rosettes (Figures 7I-7K). Only 1 out of 5 embryos electroporated with mFoxp1 and 0 out of 10 control embryos displayed this phenotype. The presence of ectopic neural rosettes demonstrates the ability of hFOXP1 to promote the neuroepithelial character of aRG.

To further assess the progenitor-promoting ability of mFoxp1 and hFOXP1, we assessed cortices one-week post-electroporation (P0.5) for the presence of GFP$^+$ cells expressing Pax6. In control electroporations, we did not detect the presence of GFP$^+$ Pax6$^+$ cells except for a very small number in the VZ. However, after electroporation with mFoxp1/hFOXP1 vectors, we detected an 8 and 6-fold increase in GFP$^+$ Pax6$^+$ cells in the VZ, respectively (Figures 7O-7Q, 7X), indicating aRG retention within the postnatal VZ. In addition, a significant number of GFP$^+$ Pax6$^+$ were detected outside of the VZ in the CP (Figures 7L-7N, 7Y), suggesting long term maintenance of a progenitor population upon misexpression of mouse and human Foxp1.

Given the association between FOXP1 and human bRG we asked whether ectopic Pax6$^+$ cells present after misexpression of mFoxp1/hFOXP1 represented a population of bRG. To begin, we quantified coexpression of the bRG marker Sox2 within ectopic Pax6$^+$/GFP$^+$ cells. In control electroporations, we found an average of 0.34 Sox2$^+$/Pax6$^+$/GFP$^+$ cells/300μm^2 (Figures 7R, 7Z). Following Foxp1 electroporation, there were significant increases in the number of ectopic Sox2$^+$/Pax6$^+$/GFP$^+$ cells, with a ~9-fold change seen with mFoxp1 and ~10-fold change with hFOXP1 (Figures 7S-7T, 7Z, 7AA).

Morphologically, bRG are distinct from aRG and other cell types found in the cortex; they possess a simple basal process projecting towards the pial surface. To analyze the morphology of ectopic GFP$^+$ Pax6$^+$ cells, we co-electroporated control, mFoxp1 or hFOXP1 plasmids along with a membrane bound (mb) GFP construct into the E13.5 mouse cortex and collected pups for analysis at P0.5. With control electroporations, we did not identify any GFP$^+$ cells that resembled bRG. A small number of GFP$^+$ cells with an elaborate basal process were detected; however, these cells resembled neurons with basal dendrites (Figures 7U, S9D-S9G). Additionally, these cells did not express Pax6 (Figure 7U) but rather expressed Myt1l (Figure S9D) and a number of spatially appropriate subtype markers (Tbr1, Ctip2, Cux1 or Lhx2) (Figures S9E-S9G), confirming their neuronal identity. By contrast, cortices electroporated with mFoxp1/hFOXP1 constructs displayed abventricular GFP$^+$ cells that morphologically resembled bRG with a simple basal process (Figures 8V, 8W, and S8H-S8M; see also Hansen et al., 2010). Nearly all of these GFP$^+$ cells expressed Pax6, though we did not observe expression of markers associated with human bRG such as HOPX or ITGB5. A few GFP$^+$ cells in these electroporated cortices were found to express Myt1l albeit at varying levels (Figures S9H, S9K), though none were found to express specific neuronal markers such as Tbr1, Ctip2, Cux1 or Lhx2 (Figures S9I, S9L, S9J, S9M). Together, these data demonstrate that mFoxp1/hFOXP1 misexpression not only promotes aRG maintenance but can also promote the formation of cells with some of the molecular and morphological characteristics of bRG.

DISCUSSION

The progressive generation of neuronal subtypes in the cortex depends on the maintenance of a pool of proliferating progenitors and their timely differentiation into early born DL and late born SL neurons. Our studies identify Foxp1 as a critical regulator of these processes, acting to promote self-renewing divisions that expand the aRG progenitor pool, while also favoring the generation of early-born DL neurons. The cessation of early neurogenesis

requires Foxp1 downregulation, suggesting that its expression and activity helps define distinct windows of corticogenesis. The contributions of Foxp1 appear to be even more extensive in humans, as its expression is prominently associated with the early formation and proliferative expansion of bRG, raising the possibility that its progenitor maintenance functions may have been co-opted to facilitate the expansion of brain size across species. These observations may further explain how FOXP1 mutation in humans leads to a spectrum of neurodevelopmental defects.

Foxp1 and the temporal competency model for corticogenesis

Neural progenitor transplantation studies, in vitro cell lineage analyses, and in vivo fate mapping experiments have all indicated that there is a window of plasticity during early neurogenesis in which aRG are competent to give rise to all cortical neuron subtypes (Desai and McConnell, 2000; Shen et al., 2006; Gao et al., 2014; Ma et al., 2018). This temporal competence model predicts that there are factors expressed by early aRG that promote NSC maintenance and bias the production of early born DL neurons. As neurogenesis proceeds, the actions of these factors would need to be reduced or counterbalanced by opposing factors to enact a switch to late SL neurogenesis. Indeed, several factors have been implicated in this switching process including for early fates: Otx1, Foxg1, CoupTF1I/II, Fezf2 and Ikaros (Frantz and McConnell, 1996; Okano and Temple, 2009; Tuoc et al., 2009; Alsio et al., 2013; Guo et al., 2013; Toma and Hanashima, 2015), and Brn1/2 and Cux1/2 for later fates (Franco et al., 2012; Dominguez et al., 2013). However, most of these factors appear to exhibit some but not all of the cardinal features of a temporal determinant, namely restricted expression in progenitors during defined time windows of neurogenesis, a requirement for that phase of neurogenesis, and a capacity to alter the intervals of neuron production when misexpressed. In this regard, Foxp1 stands out as an intriguing candidate as its expression demarcates the period of DL neuron production, and its function is both necessary and sufficient for this process.

Our electroporation experiments show that acute misexpression of Foxp1 in aRG during the time window of late neurogenesis can elicit the generation of early born neurons including DL neurons and the earliest born Layer I cells. Similar results were observed in transgenic Foxp1^{ON} mice, where DL neurons continued to be generated at later stages of embryogenesis and early postnatal life. However, despite the extended production of DL cells, SL neurogenesis and gliogenesis nevertheless continued in the face of ectopic Foxp1 expression. These findings suggest that while Foxp1 can broaden the neurogenic competence of aRG, its functions do not prohibit formation of later born cell types. Supporting this conclusion, forced expression of Foxp1 in postmitotic neurons using Nex1^{Cre}-mediated recombination neither stimulated the formation of DL neurons nor blocked SL fates.

Multipotency and broad neurogenic competence are characteristic features of early aRG. Our data show that early aRG express high levels of Foxp1, which can stimulate symmetric cell divisions and progenitor expansion, while also promoting the assignment of DL fates. Analyses of Foxp1^{OFF} mice demonstrate that the later stages of neurogenesis and gliogenesis were unaffected by the loss of Foxp1, presumably reflecting the endogenous

downregulation of Foxp1 and the proposition that Foxp1 does not function in late aRG. These lines of evidence together suggest that Foxp1 both ensures the plasticity required by aRG during early neurogenesis and act as a key factor in the regulation of temporal competency.

Potential downstream targets of Foxp1 in corticogenesis

Foxp1 exhibits diverse activities in the developing CNS, reflecting the different cell types in which it is expressed and phases of differentiation with which it is associated. The downstream targets of Foxp1 in aRG remain unclear; however, in postnatal cortical neurons Foxp1 can repress genes involved in neurogenesis, neuronal migration, and synaptogenesis (Usui et al., 2017). Similarly, studies using cultured late stage cortical progenitors and differentiated neurons have proposed that Foxp1 directly represses the Notch receptor ligand Jagged1 to promote neuronal differentiation (Braccioli et al., 2017).

The ability of Foxp1 to promote aRG maintenance suggests that some of its key targets likely include factors that stimulate cell differentiation as well as those that control self-renewal. Previous studies have demonstrated that self-renewal tracks with vertical divisions and that randomizing spindle angle favors basal progenitor and neuron production (Konno et al., 2008). Potentially, high levels of Foxp1 in early aRG could be involved in the repression of factors such as Inscutable that can disrupt the mitotic spindle (Lancaster and Knoblich, 2012; Paridaen and Huttner, 2014) and thereby promote vertical divisions. Our paired cell assays also demonstrate that concomitant with an increase in vertical divisions, cells expressing Foxp1 were biased toward aRG-aRG symmetric self-renewal. The ability of Foxp1 to promote symmetric self-renewing divisions ex vivo suggests it could act through a cell intrinsic mechanism.

One factor that was consistently impacted by Foxp1 gain and loss was Pax6, one of the earliest markers of cortical progenitors. Pax6 expression is maintained in aRG throughout embryonic neurogenesis and is also utilized by progenitor cells in the SVZ of the postnatal and adult forebrain. In humans and non-human primates, Pax6 is also associated with bRG cells. At each stage of development, Foxp1 misexpression substantially increased Pax6 levels suggesting that many of its progenitor-promoting activities could be attributed to this induction. There are striking similarities in the consequences of *Pax6* and *Foxp1* deletions, as mice lacking either gene exhibit more oblique/horizontal divisions, reduced aRG proliferation, and, at later stages, decreased neuron production (Ypsilanti and Rubenstein, 2016). Ectopic Pax6 expression can also impede neuronal differentiation and induce the formation of bRG-like cells in the mouse (Wong et al., 2015). Interestingly, our electroporation data suggest that preservation or elevation of Pax6 expression through Foxp1 misexpression is not alone sufficient to promote all aspects bRG character, suggesting that additional factors are required to fully impart bRG identity.

Contributions of Foxp1 to human cortical development

Significant progress has been made comparing the transcriptomic landscapes of human and mouse cortical progenitors (Florio et al., 2015; Johnson et al., 2015; Pollen et al., 2015). These analyses have identified valuable bRG markers and provided insights into how human

bRG are regulated and what distinguishes them from other progenitor populations. However, to date, few factors have been identified that differentiate between mouse and human bRG. Our studies show that Foxp1 is not expressed in mouse bRG but is prominently expressed in human bRG, particularly during the early phase of corticogenesis. Comparisons of mouse and human bRG have demonstrated that mouse bRG are less proliferative, have a reduced capacity for self-renewal, and are transcriptionally comparable to IP whereas human bRG most closely resemble aRG (Johnson et al., 2015).

Little is currently known about the mechanisms that regulate bRG formation and expansion to create the enlarged oSVZ progenitor compartment seen in the human and non-human primate brain. Our analyses have demonstrated that in mouse, Foxp1 manipulation can influence the generation of basal $Pax6^+$ $Tbr2^-$ basal progenitors. Taken together with our expression analysis of FOXP1 in developing human cortex, we suggest that Foxp1 could contribute to these processes. When ectopically expressed in the mouse cortex at mid-neurogenesis, Foxp1 elicited the formation of basal $Pax6^+$ cells. Analysis of electroporated cortices at P0.5 demonstrated that while the majority of transfected cells differentiate into neurons, a significant number of cells misexpressing Foxp1 continue to express Pax6. Moreover, a subset of these basal $Foxp1^+$ $Pax6^+$ cells also express Sox2, another characteristic feature of bRG, for at least a week after electroporation. Some of these Foxp1-transfected cells further exhibited bRG-like morphologies; however, they did not express other bRG markers. It should be noted that many markers used to identify bRG were first identified in human and their expression in mouse bRG has not been well documented. An alternative interpretation of our findings is that while Foxp1 expression can elicit the formation of cells with bRG-like characteristics, it is not alone sufficient to drive the process to completion. Further studies are required to understand the role of Foxp1 in human cortical progenitors and its potential role in bRG generation and expansion.

Pathological implications of Foxp1 dysregulation

Foxp genes are members of the evolutionarily ancient Fox family, and their activities have been linked to the acquisition of human specific traits such as language, speech and intellectual capabilities (Hannenhalli and Kaestner, 2009). However, a consequence of the selective pressures that permitted language and cognition in humans also made us vulnerable to cognitive disorders such as intellectual disability and ASD (Lepp et al., 2013). Copy number variants, haploinsufficiencies and de novo point mutations in *FOXP1* have been found in patients exhibiting ASD and speech impairment (Hamdan et al., 2010; Horn et al., 2010; O'Roak et al., 2011; Le Fevre et al., 2013; Meerschaut et al., 2017). Intriguingly, increased expression of *FOXP1* has also been reported in patients with ASD (Chien et al., 2013).

Mouse models have linked Foxp1 in striatal neurons with ASD-like behavior and transcriptional regulation of autism-related pathways (Araujo et al., 2015; Bacon et al., 2015). Next generation sequencing studies further show that many genes implicated in ASD are highly coexpressed during human cortical development and can be grouped into modules that involve distinct biological functions including early transcriptional regulation (Parikshak et al., 2015). These studies underscore the importance of understanding the spatial and

temporal context of specific ASD susceptibility genes in order to ascertain their role in brain development. Much of the research involving Foxp1 and human neurodevelopmental disorders has thus far focused on the functions of Foxp1 in postmitotic neurons. Our findings that experimentally induced changes in Foxp1 levels can alter the maintenance of neural progenitors, time windows of DL vs. SL neurogenesis, and to some extent production of bRG suggest other means by which Foxp1 mutations could impact the growth, cytoarchitecture, and evolution of the human cerebral cortex.

STAR METHODS

LEAD CONTACT AND MATERIALS AVAILABILITY.

Further information and requests for resources and reagents should be directed to and will be fulfilled by the Lead Contact, Bennett Novitch (bnovitch@ucla.edu). This study did not generate new unique reagents.

EXPERIMENTAL MODEL AND SUBJECT DETAILS

Animal preparation and tissue analysis—$Foxp1a^{Tg/+}$, $Foxp1^{fl/fl}$, $Emx1^{Cre(KI)/+}$, $Emx1^{Cre(Tg)/+}$, and $Nex1^{Cre/+}$ mice were maintained as previously described (Gorski et al., 2002; Iwasato et al., 2004; Goebbels et al., 2006; Feng et al., 2010; Wang et al., 2014) following UCLA Chancellor's Animal Research Committee husbandry guidelines. Embryonic cortices were fixed in 4% paraformaldehyde overnight. Postnatal and adult animals were perfused according to UCLA guidelines, and brains were fixed overnight. Tissues were cryosectioned and processed for immunohistochemistry or in situ hybridization as previously described (Pearson et al., 2011; Rousso et al., 2012). Primary antibodies are listed in the Key Resources table. A probe against the 5'UTR of mouse *Foxp1* was generated using PCR.

Human brain tissue—Experiments were performed with prior approval from the research ethics committees at the UCLA Office of the Human Research Protection Program, the University of Tübingen (institutional review board [IRB]#323/2017BO2), and Novogenix Laboratories. Tissues were obtained with informed consent as discarded materials resulting from elective legal terminations. Samples were de-identified in accordance with institutional guidelines. Specimen ages for this study are denoted as gestational weeks as determined by the date of the last menstrual period or ultrasound and confirmed by analysis of developmental characteristics. Samples were processed as previously described (Watanabe et al., 2017).

METHODS DETAILS

BrdU incorporation analyses.—Pregnant dams were given intraperitoneal injections with a volume of BrdU based on the weight of the mouse; 100μg BrdU/gram of body weight. Embryos were collected 2 hours, at E18.5 or P1.5. For staining analyses, tissue cryosections were treated with 4% PFA for ten minutes and 4N HCl for 5 minutes prior to antibody labeling.

Cortical progenitor paired cell assays.—Lateral cortex tissue from E13.5 embryos was collected and cells dissociated, plated and cultured for 20 hours as previously described (Qian et al., 2000).

Plasmid expression constructs.—Generation of mouse and human Foxp1 expression vectors was conducted as previously described (Rousso et al., 2008; Adams et al., 2015). In brief, the coding region of each gene was amplified by PCR and cloned into a Gateway compatible version of the pCIG expression vector, which carries an IRES-nuclear-EGFP reporter (Megason and McMahon, 2002).

In utero electroporation.—Electroporations were performed as previously described (Cruz-Martin et al., 2010). A solution containing 1.0μg/μL of plasmid DNA (pCIG or pCIG-Foxp1) and 0.05% Fast Green was injected in the left telencephalic vesicle at E13.5, and 5 square electric pulses (40V, 50 ms long) were delivered at 500 ms intervals using a BTX Harvard Instruments electroporator. Brains were recovered at E15.5 or at birth (P0.5), fixed in 4% paraformaldehyde, cryosectioned, and used for immunohistochemical staining analysis.

Microscope Imaging.—Confocal images were acquired using Zeiss LSM 780 or LSM 800 confocal microscopes and Zen blue or black software. DIC imaging of in situ hybridizations were collected using a Zeiss Axioimager microscope and Axiovision software. Images were processed and compiled using Adobe Photoshop with image adjustments applied to the entire image and restricted to brightness, contrast and levels. Images shown in figures as comparisons, e.g. intensity levels, were obtained and processed in parallel using identical settings. Composite images were assembled using Adobe Illustrator software.

QUANTIFICATION AND STATISTICAL ANALYSES

Cell and protein staining quantification.—For each experiment, the number of labeled lateral cortex cells within a ~200 μm x radial width area per section was quantified from 4-5 16 μm sections sampled at ~100 μm intervals along the rostrocaudal axis within the presumptive somatosensory region of the cortex. The number of cells in each Foxp1 condition was normalized to littermate control embryos. For electroporation experiments, GFP$^+$ cells were counted and the percentage of those cells expressing specific markers calculated. For BrdU birthdating experiments, the total number of BrdU$^+$ cells within either Layer VI or II/III-IV were counted and the percentage of BrdU$^+$/Tbr1$^+$ or Lhx2$^+$ cells calculated. For the later embryonic incorporation experiments, the total number of BrdU$^+$ cells in the CP were counted and the number of double positive cells quantified. For mitotic division angle analyses, high magnification images of dividing cells in anaphase along the ventricular wall were taken and angle was measured relative to apical surface. Between 80-100 cells per condition were measured. For Pair cell assays, 200-400 couplets per embryo were analyzed and the percentage of total couplets representing each division type calculated. Intensity values relative to background staining were measured using Fiji software, using images from each condition that were measured using identical settings.

Statistical Analyses.—The normality of each data set was determined using Graphpad Prism software and the appropriate parametric (normal distribution) or non-parametric (uneven distribution) test was applied as indicated in the Figure legends. One-way ANOVA (with post-hoc multiple comparison test), Student's t-test, and Mann-Whitney *U*-tests were calculated using Prism software. Wilcoxon signed rank test was applied in the case where control values were identical (Figure S5B). Significance was assumed when $p < 0.05$. The results of statistical tests (p values and sample sizes) are reported in Table S1. Signifiers used are as follows: $p > 0.05$, ns; * p   0.05; ** p   0.01; *** p   0.001; **** p   0.0001. Unless otherwise indicated, all data are presented as mean ± SEM.

DATA AND CODE AVAILABILITY.

The datasets supporting the current study have not been deposited but are available upon request from the corresponding author.

Supplementary Material

Refer to Web version on PubMed Central for supplementary material.

ACKNOWLEDGEMENTS

REFERENCES

Adams KL, Rousso DL, Umbach JA, and Novitch BG (2015). Foxp1-mediated programming of limb-innervating motor neurons from mouse and human embryonic stem cells. Nat Commun 6, 6778. [PubMed: 25868900]

Alsio JM, Tarchini B, Cayouette M, and Livesey FJ (2013). Ikaros promotes early-born neuronal fates in the cerebral cortex. Proc Natl Acad Sci U S A 110, E716–725. [PubMed: 23382203]

Araujo DJ, Anderson AG, Berto S, Runnels W, Harper M, Ammanuel S, Rieger MA, Huang HC, Rajkovich K, Loerwald KW, et al. (2015). FoxP1 orchestration of ASD-relevant signaling pathways in the striatum. Genes Dev 29, 2081–2096. [PubMed: 26494785]

Bacon C, Schneider M, Le Magueresse C, Froehlich H, Sticht C, Gluch C, Monyer H, and Rappold GA (2015). Brain-specific Foxp1 deletion impairs neuronal development and causes autistic-like behaviour. Mol Psychiatry 20, 632–639. [PubMed: 25266127]

Bae BI, Jayaraman D, and Walsh CA (2015). Genetic changes shaping the human brain. Dev Cell 32, 423–434. [PubMed: 25710529]

Braccioli L, Vervoort SJ, Adolfs Y, Heijnen CJ, Basak O, Pasterkamp RJ, Nijboer CH, and Coffer PJ (2017). FOXP1 Promotes Embryonic Neural Stem Cell Differentiation by Repressing Jagged1 Expression. Stem Cell Reports 9, 1530–1545. [PubMed: 29141232]

Chien WH, Gau SS, Chen CH, Tsai WC, Wu YY, Chen PH, Shang CY, and Chen CH (2013). Increased gene expression of FOXP1 in patients with autism spectrum disorders. Mol Autism 4, 23. [PubMed: 23815876]

Dasen JS, De Camilli A, Wang B, Tucker PW, and Jessell TM (2008). Hox repertoires for motor neuron diversity and connectivity gated by a single accessory factor, FoxP1. Cell 134, 304–316. [PubMed: 18662545]

Desai AR, and McConnell SK (2000). Progressive restriction in fate potential by neural progenitors during cerebral cortical development. Development 127, 2863–2872. [PubMed: 10851131]

Dominguez MH, Ayoub AE, and Rakic P (2013). POU-III transcription factors (Brn1, Brn2, and Oct6) influence neurogenesis, molecular identity, and migratory destination of upper-layer cells of the cerebral cortex. Cereb Cortex 23, 2632–2643. [PubMed: 22892427]

Dwyer ND, Chen B, Chou SJ, Hippenmeyer S, Nguyen L, and Ghashghaei HT (2016). Neural Stem Cells to Cerebral Cortex: Emerging Mechanisms Regulating Progenitor Behavior and Productivity. J Neurosci 36, 11394–11401. [PubMed: 27911741]

Ernst C (2016). Proliferation and Differentiation Deficits are a Major Convergence Point for Neurodevelopmental Disorders. Trends Neurosci 39, 290–299. [PubMed: 27032601]

Feng X, Ippolito GC, Tian L, Wiehagen K, Oh S, Sambandam A, Willen J, Bunte RM, Maika SD, Harriss JV, et al. (2010). Foxp1 is an essential transcriptional regulator for the generation of quiescent naive T cells during thymocyte development. Blood 115, 510–518. [PubMed: 19965654]

Ferland RJ, Cherry TJ, Preware PO, Morrisey EE, and Walsh CA (2003). Characterization of Foxp2 and Foxp1 mRNA and protein in the developing and mature brain. J Comp Neurol 460, 266–279. [PubMed: 12687690]

Florio M, Albert M, Taverna E, Namba T, Brandl H, Lewitus E, Haffner C, Sykes A, Wong FK, Peters J, et al. (2015). Human-specific gene ARHGAP11B promotes basal progenitor amplification and neocortex expansion. Science 347, 1465–1470. [PubMed: 25721503]

Florio M, and Huttner WB (2014). Neural progenitors, neurogenesis and the evolution of the neocortex. Development 141, 2182–2194. [PubMed: 24866113]

Franco SJ, Gil-Sanz C, Martinez-Garay I, Espinosa A, Harkins-Perry SR, Ramos C, and Muller U (2012). Fate-restricted neural progenitors in the mammalian cerebral cortex. Science 337, 746–749. [PubMed: 22879516]

Franco SJ, and Muller U (2013). Shaping our minds: stem and progenitor cell diversity in the mammalian neocortex. Neuron 77, 19–34. [PubMed: 23312513]

Frantz GD, and McConnell SK (1996). Restriction of late cerebral cortical progenitors to an upper-layer fate. Neuron 17, 55–61. [PubMed: 8755478]

Gao P, Postiglione MP, Krieger TG, Hernandez L, Wang C, Han Z, Streicher C, Papusheva E, Insolera R, Chugh K, et al. (2014). Deterministic progenitor behavior and unitary production of neurons in the neocortex. Cell 159, 775–788. [PubMed: 25417155]

Goebbels S, Bormuth I, Bode U, Hermanson O, Schwab MH, and Nave KA (2006). Genetic targeting of principal neurons in neocortex and hippocampus of NEX-Cre mice. Genesis 44, 611–621. [PubMed: 17146780]

Gorski JA, Talley T, Qiu M, Puelles L, Rubenstein JL, and Jones KR (2002). Cortical excitatory neurons and glia, but not GABAergic neurons, are produced in the Emx1-expressing lineage. J Neurosci 22, 6309–6314. [PubMed: 12151506]

Greig LC, Woodworth MB, Galazo MJ, Padmanabhan H, and Macklis JD (2013). Molecular logic of neocortical projection neuron specification, development and diversity. Nat Rev Neurosci 14, 755–769. [PubMed: 24105342]

Groszer M, Keays DA, Deacon RM, de Bono JP, Prasad-Mulcare S, Gaub S, Baum MG, French CA, Nicod J, Coventry JA, et al. (2008). Impaired synaptic plasticity and motor learning in mice with a point mutation implicated in human speech deficits. Curr Biol 18, 354–362. [PubMed: 18328704]

Guo C, Eckler MJ, McKenna WL, McKinsey GL, Rubenstein JL, and Chen B (2013). Fezf2 expression identifies a multipotent progenitor for neocortical projection neurons, astrocytes, and oligodendrocytes. Neuron 80, 1167–1174. [PubMed: 24314728]

Hamdan FF, Daoud H, Rochefort D, Piton A, Gauthier J, Langlois M, Foomani G, Dobrzeniecka S, Krebs MO, Joober R, et al. (2010). De novo mutations in FOXP1 in cases with intellectual disability, autism, and language impairment. Am J Hum Genet 87, 671–678. [PubMed: 20950788]

Hannenhalli S, and Kaestner KH (2009). The evolution of Fox genes and their role in development and disease. Nat Rev Genet 10, 233–240. [PubMed: 19274050]

Hansen DV, Lui JH, Parker PR, and Kriegstein AR (2010). Neurogenic radial glia in the outer subventricular zone of human neocortex. Nature 464, 554–561. [PubMed: 20154730]

Hisaoka T, Nakamura Y, Senba E, and Morikawa Y (2010). The forkhead transcription factors, Foxp1 and Foxp2, identify different subpopulations of projection neurons in the mouse cerebral cortex. Neuroscience 166, 551–563. [PubMed: 20040367]

Horn D, Kapeller J, Rivera-Brugues N, Moog U, Lorenz-Depiereux B, Eck S, Hempel M, Wagenstaller J, Gawthrope A, Monaco AP, et al. (2010). Identification of FOXP1 deletions in three unrelated patients with mental retardation and significant speech and language deficits. Hum Mutat 31, E1851–1860. [PubMed: 20848658]

Hu H, Wang B, Borde M, Nardone J, Maika S, Allred L, Tucker PW, and Rao A (2006). Foxp1 is an essential transcriptional regulator of B cell development. Nat Immunol 7, 819–826. [PubMed: 16819554]

Iwasato T, Nomura R, Ando R, Ikeda T, Tanaka M, and Itohara S (2004). Dorsal telencephalon-specific expression of Cre recombinase in PAC transgenic mice. Genesis 38, 130–138. [PubMed: 15048810]

Johnson MB, Wang PP, Atabay KD, Murphy EA, Doan RN, Hecht JL, and Walsh CA (2015). Single-cell analysis reveals transcriptional heterogeneity of neural progenitors in human cortex. Nat Neurosci 18, 637–646. [PubMed: 25734491]

Konno D, Shioi G, Shitamukai A, Mori A, Kiyonari H, Miyata T, and Matsuzaki F (2008). Neuroepithelial progenitors undergo LGN-dependent planar divisions to maintain self-renewability during mammalian neurogenesis. Nat Cell Biol 10, 93–101. [PubMed: 18084280]

Kwan KY, Sestan N, and Anton ES (2012). Transcriptional co-regulation of neuronal migration and laminar identity in the neocortex. Development 139, 1535–1546. [PubMed: 22492350]

Lai CS, Fisher SE, Hurst JA, Vargha-Khadem F, and Monaco AP (2001). A forkhead-domain gene is mutated in a severe speech and language disorder. Nature 413, 519–523. [PubMed: 11586359]

Lancaster MA, and Knoblich JA (2012). Spindle orientation in mammalian cerebral cortical development. Curr Opin Neurobiol 22, 737–746. [PubMed: 22554882]

Le Fevre AK, Taylor S, Malek NH, Horn D, Carr CW, Abdul-Rahman OA, O'Donnell S, Burgess T, Shaw M, Gecz J, et al. (2013). FOXP1 mutations cause intellectual disability and a recognizable phenotype. Am J Med Genet A 161A, 3166–3175. [PubMed: 24214399]

Lepp S, Anderson A, and Konopka G (2013). Connecting signaling pathways underlying communication to ASD vulnerability. Int Rev Neurobiol 113, 97–133. [PubMed: 24290384]

Lim DA, and Alvarez-Buylla A (2016). The Adult Ventricular-Subventricular Zone (V-SVZ) and Olfactory Bulb (OB) Neurogenesis. Cold Spring Harb Perspect Biol 8.

Lui JH, Hansen DV, and Kriegstein AR (2011). Development and evolution of the human neocortex. Cell 146, 18–36. [PubMed: 21729779]

Ma J, Shen Z, Yu YC, and Shi SH (2018). Neural lineage tracing in the mammalian brain. Curr Opin Neurobiol 50, 7–16. [PubMed: 29125960]

Mall M, Kareta MS, Chanda S, Ahlenius H, Perotti N, Zhou B, Grieder SD, Ge X, Drake S, Euong Ang C, et al. (2017). Myt1l safeguards neuronal identity by actively repressing many non-neuronal fates. Nature 544, 245–249. [PubMed: 28379941]

Meerschaut I, Rochefort D, Revencu N, Petre J, Corsello C, Rouleau GA, Hamdan FF, Michaud JL, Morton J, Radley J, et al. (2017). FOXP1-related intellectual disability syndrome: a recognisable entity. J Med Genet 54, 613–623. [PubMed: 28735298]

Megason SG, and McMahon AP (2002). A mitogen gradient of dorsal midline Wnts organizes growth in the CNS. Development 129, 2087–2098. [PubMed: 11959819]

Nowakowski TJ, Pollen AA, Sandoval-Espinosa C, and Kriegstein AR (2016). Transformation of the Radial Glia Scaffold Demarcates Two Stages of Human Cerebral Cortex Development. Neuron 91, 1219–1227. [PubMed: 27657449]

O'Roak BJ, Deriziotis P, Lee C, Vives L, Schwartz JJ, Girirajan S, Karakoc E, Mackenzie AP, Ng SB, Baker C, et al. (2011). Exome sequencing in sporadic autism spectrum disorders identifies severe de novo mutations. Nat Genet 43, 585–589. [PubMed: 21572417]

Okano H, and Temple S (2009). Cell types to order: temporal specification of CNS stem cells. Curr Opin Neurobiol 19, 112–119. [PubMed: 19427192]

Ortiz-Alvarez G, Daclin M, Shihavuddin A, Lansade P, Fortoul A, Faucourt M, Clavreul S, Lalioti ME, Taraviras S, Hippenmeyer S, et al. (2019). Adult Neural Stem Cells and Multiciliated Ependymal Cells Share a Common Lineage Regulated by the Geminin Family Members. Neuron 102, 159–172.e157. [PubMed: 30824354]

Paridaen JT, and Huttner WB (2014). Neurogenesis during development of the vertebrate central nervous system. EMBO Rep 15, 351–364. [PubMed: 24639559]

Parikshak NN, Gandal MJ, and Geschwind DH (2015). Systems biology and gene networks in neurodevelopmental and neurodegenerative disorders. Nat Rev Genet 16, 441–458. [PubMed: 26149713]

Pearson CA, Ohyama K, Manning L, Aghamohammadzadeh S, Sang H, and Placzek M (2011). FGF-dependent midline-derived progenitor cells in hypothalamic infundibular development. Development 138, 2613–2624. [PubMed: 21610037]

Pollen AA, Nowakowski TJ, Chen J, Retallack H, Sandoval-Espinosa C, Nicholas CR, Shuga J, Liu SJ, Oldham MC, Diaz A, et al. (2015). Molecular identity of human outer radial glia during cortical development. Cell 163, 55–67. [PubMed: 26406371]

Qian X, Shen Q, Goderie SK, He W, Capela A, Davis AA, and Temple S (2000). Timing of CNS cell generation: a programmed sequence of neuron and glial cell production from isolated murine cortical stem cells. Neuron 28, 69–80. [PubMed: 11086984]

Redmond SA, Figueres-Onate M, Obernier K, Nascimento MA, Parraguez JI, Lopez-Mascaraque L, Fuentealba LC, and Alvarez-Buylla A (2019). Development of Ependymal and Postnatal Neural Stem Cells and Their Origin from a Common Embryonic Progenitor. Cell Rep 27, 429–441.e423. [PubMed: 30970247]

Rousso DL, Gaber ZB, Wellik D, Morrisey EE, and Novitch BG (2008). Coordinated actions of the forkhead protein Foxp1 and Hox proteins in the columnar organization of spinal motor neurons. Neuron 59, 226–240. [PubMed: 18667151]

Rousso DL, Pearson CA, Gaber ZB, Miquelajauregui A, Li S, Portera-Cailliau C, Morrisey EE, and Novitch BG (2012). Foxp-mediated suppression of N-cadherin regulates neuroepithelial character and progenitor maintenance in the CNS. Neuron 74, 314–330. [PubMed: 22542185]

Sanders SJ, He X, Willsey AJ, Ercan-Sencicek AG, Samocha KE, Cicek AE, Murtha MT, Bal VH, Bishop SL, Dong S, et al. (2015). Insights into Autism Spectrum Disorder Genomic Architecture and Biology from 71 Risk Loci. Neuron 87, 1215–1233. [PubMed: 26402605]

Shen Q, Wang Y, Dimos JT, Fasano CA, Phoenix TN, Lemischka IR, Ivanova NB, Stifani S, Morrisey EE, and Temple S (2006). The timing of cortical neurogenesis is encoded within lineages of individual progenitor cells. Nat Neurosci 9, 743–751. [PubMed: 16680166]

Shu W, Lu MM, Zhang Y, Tucker PW, Zhou D, and Morrisey EE (2007). Foxp2 and Foxp1 cooperatively regulate lung and esophagus development. Development 134, 1991–2000. [PubMed: 17428829]

Taverna E, Gotz M, and Huttner WB (2014). The cell biology of neurogenesis: toward an understanding of the development and evolution of the neocortex. Annu Rev Cell Dev Biol 30, 465–502. [PubMed: 25000993]

Toma K, and Hanashima C (2015). Switching modes in corticogenesis: mechanisms of neuronal subtype transitions and integration in the cerebral cortex. Front Neurosci 9, 274. [PubMed: 26321900]

Tuoc TC, Radyushkin K, Tonchev AB, Pinon MC, Ashery-Padan R, Molnar Z, Davidoff MS, and Stoykova A (2009). Selective cortical layering abnormalities and behavioral deficits in cortex-specific Pax6 knock-out mice. J Neurosci 29, 8335–8349. [PubMed: 19571125]

Usui N, Araujo DJ, Kulkarni A, Co M, Ellegood J, Harper M, Toriumi K, Lerch JP, and Konopka G (2017). Foxp1 regulation of neonatal vocalizations via cortical development. Genes Dev 31, 2039–2055. [PubMed: 29138280]

Wang B, Weidenfeld J, Lu MM, Maika S, Kuziel WA, Morrisey EE, and Tucker PW (2004). Foxp1 regulates cardiac outflow tract, endocardial cushion morphogenesis and myocyte proliferation and maturation. Development 131, 4477–4487. [PubMed: 15342473]

Wang H, Geng J, Wen X, Bi E, Kossenkov AV, Wolf AI, Tas J, Choi YS, Takata H, Day TJ, et al. (2014). The transcription factor Foxp1 is a critical negative regulator of the differentiation of follicular helper T cells. Nat Immunol 15, 667–675. [PubMed: 24859450]

Watanabe M, Buth JE, Vishlaghi N, de la Torre-Ubieta L, Taxidis J, Khakh BS, Coppola G, Pearson CA, Yamauchi K, Gong D, et al. (2017). Self-Organized Cerebral Organoids with Human-Specific Features Predict Effective Drugs to Combat Zika Virus Infection. Cell Rep 21, 517–532. [PubMed: 29020636]

Wong FK, Fei JF, Mora-Bermudez F, Taverna E, Haffner C, Fu J, Anastassiadis K, Stewart AF, and Huttner WB (2015). Sustained Pax6 Expression Generates Primate-like Basal Radial Glia in Developing Mouse Neocortex. PLoS Biol 13, e1002217. [PubMed: 26252244]

Young KM, Fogarty M, Kessaris N, and Richardson WD (2007). Subventricular zone stem cells are heterogeneous with respect to their embryonic origins and neurogenic fates in the adult olfactory bulb. J Neurosci 27, 8286–8296. [PubMed: 17670975]

Ypsilanti AR, and Rubenstein JL (2016). Transcriptional and epigenetic mechanisms of early cortical development: An examination of how Pax6 coordinates cortical development. J Comp Neurol 524, 609–629. [PubMed: 26304102]

HIGHLIGHTS

- Foxp1 is transiently expressed by aRG during the early phase of corticogenesis

- Foxp1 promotes self-renewing vertical cell divisions and aRG maintenance

- Foxp1 gates the time window of deep layer neurogenesis

- FOXP1 is prominently associated with aRG and bRG expansion in the human neocortex
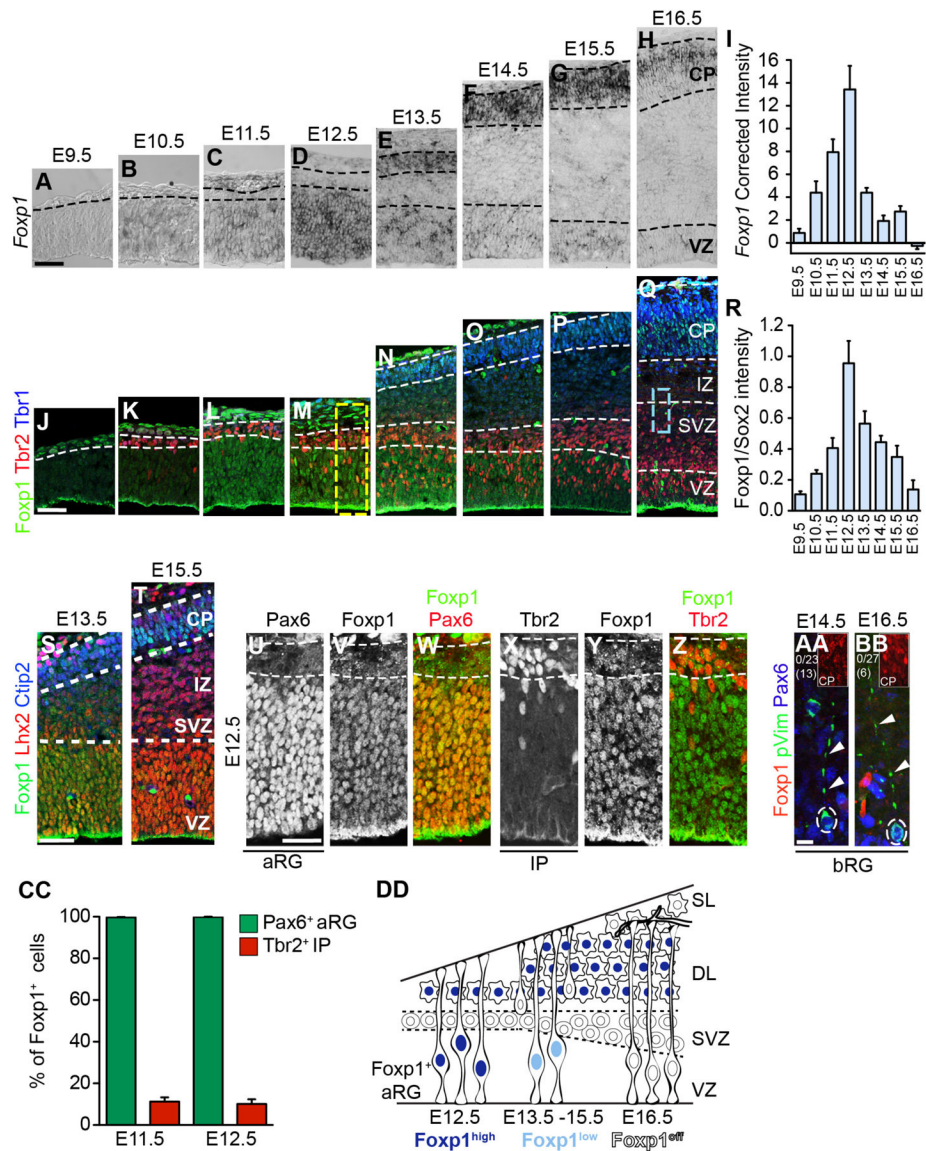
Figure 1. Foxp1 is expressed by aRG and downregulated during the transition from early to late neurogenesis.

(A-H) *Foxp1* mRNA expression in the VZ and CP during mouse cortical neurogenesis (E9.5-E16.5).

(I) Corrected intensity of *Foxp1* in the VZ (normalized to background levels). Intensity ± SEM calculated from 4 sections from 4-5 embryos per group.

(J-Q) Foxp1 protein expression in the VZ and CP (E9.5-E16.5). Tbr2 and Tbr1 immunostaining demarcate the SVZ and CP, respectively. Dashed boxes indicate areas analyzed in U-Z and AA, BB.

(R) Corrected intensity of Foxp1 protein levels (normalized to Sox2 levels). Intensity ± SEM calculated from 4 sections from 3-5 embryos per group.

(S-T) Foxp1, Ctip2 and Lhx2 expression in the cortex at E13.5 and E15.5. Dashed white lines mark boundaries of the VZ and CP.

(U-Z) Overlap of Foxp1 expression with Pax6 but not with Tbr2 at E12.5.

(AA-BB) Mouse bRG labeled with pVim and Pax6 do not express Foxp1 at E14.5 or E16.5. Arrowheads indicate basal process; white dashed circle denotes the mitotic cell soma. N = 0/23 bRG identified in 13 embryos expressed Foxp1 at E14.5. 0/27 bRG identified in 6 embryos expressed Foxp1 at E16.5. Insets show positive Foxp1 staining in cortical plate.

(CC) Percentage of Foxp1^{+} cells at E11.5 and E12.5 that express Pax6 or Tbr2. Percentage ± SEM calculated from 4 sections from 3 embryos per group.

(DD) Summary of Foxp1 expression in the VZ; high levels (dark blue) are expressed during early neurogenesis (E10.5-E12.5). Early born neurons also express Foxp1. Subsequently (E13.5-E16.5), Foxp1 levels decrease in aRG (light blue) and are absent at the onset of gliogenesis. High levels of Foxp1 are retained by deep layer neurons.

aRG, apical radial glia; bRG, basal radial glia; VZ, ventricular zone; SVZ, subventricular zone; DL, deep layers; SL, superficial layers. Scale bars; 50 μm A-T, 25 μm U-Z, 10 μm AA, BB. See also Figure S1.
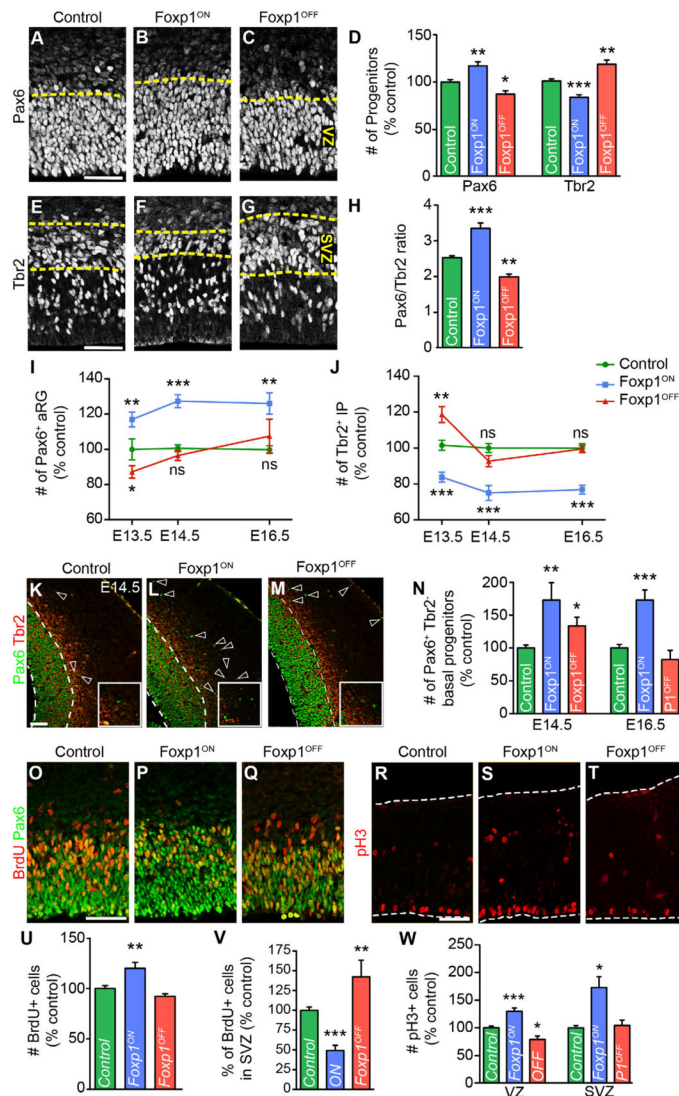
Figure 2. Foxp1 promotes radial glia identity.

(A-C) Pax6 expression in VZ aRG in E13.5 control, Foxp1ON and Foxp1OFF embryos. Yellow dashed lines mark the VZ.

(D) Number of Pax6+ aRG and Tbr2+ IP in control, Foxp1ON and Foxp1OFF embryos (% control).

(E-G) Tbr2 expression in IPs in E13.5 control, Foxp1ON and Foxp1OFF embryos. Yellow dashed lines indicate SVZ.

(H) Ratio of Pax6+ aRG to Tbr2+ IP. Mean ± SEM from at least 3 sections per embryo. N= 3 litters per genotype; 25 control embryos, 9 Foxp1ON embryos, 5 Foxp1OFF embryos (D and H).

(I-J) Number of Pax6+ aRG and Tbr2+ IP (% control) in control, Foxp1ON and Foxp1OFF embryos at E13.5, E14.5 and E16.5.

(K-M) Pax6 and Tbr2 expression at E14.5. Arrowheads indicate presence of Pax6+ Tbr2− cells outside of the VZ.

(N) Number of Pax6$^+$Tbr2$^-$ outside of the VZ (% control) at E14.5 and E16.5 in control, Foxp1^{ON} and Foxp1^{OFF} embryos. Mean ± SEM from at least 3 sections per embryo. E14.5 N= 2 litters per genotype; 16 control embryos, 6 Foxp1^{ON} embryos, 4 Foxp1^{OFF} embryos. E16.5 N= 2 litters per genotype; 5 control embryos, 5 Foxp1^{ON} embryos. 4 Foxp1^{OFF} embryos (I, J and N).

(O-Q) Co-labeling of BrdU and Pax6 in control, Foxp1^{ON} and Foxp1^{OFF} embryos at E13.5.

(R-T) Phosphorylated Histone H3 (pH3$^+$) expression in control, Foxp1^{ON} and Foxp1^{OFF} embryos at E13.5. White dashed lines mark apical and basal surfaces of the cortex.

(U) Number of BrdU$^+$ cells (% control) in control, Foxp1^{ON} and Foxp1^{OFF} embryos at E13.5.

(V) Percentage of BrdU$^+$ cells in the SVZ (% control) in control, Foxp1^{ON} and Foxp1^{OFF} embryos at E13.5.

(W) Number of pH3$^+$cells (% control) in the VZ and SVZ in E13.5 control, Foxp1^{ON} and Foxp1^{OFF} embryos. Mean ± SEM from at least 3 sections per embryo. N= 3 litters per genotype; 8 Foxp1^{ON} embryos, 12-19 control embryos, 4 Foxp1^{OFF} embryos (U, V and W). Significance determined by One-way ANOVA with post-hoc multiple comparison test, *p <0.05; **p <0.005; ***p <0.001. VZ; ventricular zone. SVZ; subventricular zone. CP; cortical plate. Scale bars; 50 μm. See also Figure S2.
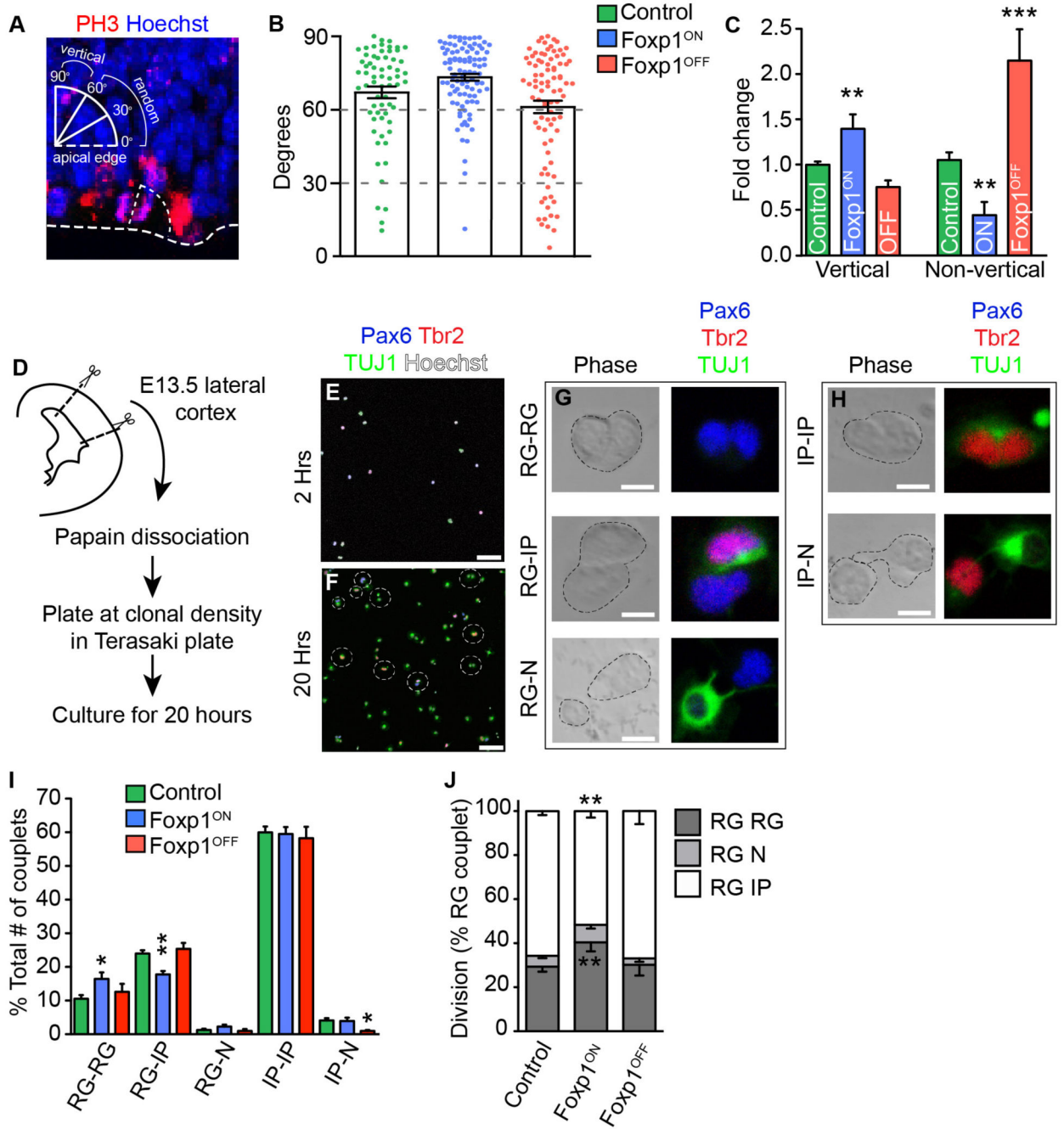
Figure 3. Foxp1 promotes vertical, symmetric self-renewing cell divisions.
(A) pH3 and Hoechst immunostaining identified dividing cells at the apical surface. Angle of division relative to the apical surface was measured in control, Foxp1[ON] and Foxp1[OFF] embryos. Vertical division 60-90°, non-vertical division 0-60°.
(B) Division angle of apical cells in control, Foxp1[ON] and Foxp1[OFF] conditions at E13.5.
(C) Fold change differences in the division angle of dividing aRG upon Foxp1 manipulation. Mean fold change ± SEM from 3 litters per genotype. N= 22 control embryos, 14 Foxp1[ON] embryos and 5 Foxp1[OFF] embryos (B and C).

(D) Schematic of pair cell assay.

(E-F) Representative images of dissociated cortical cells immunostained with Pax6, Tbr2, TUJ1 and Hoechst 2 (once cells have attached) and 20 hours after plating. Dashed circles demarcate couplets.

(G-H) Representative images of division types identified by Pax6, Tbr2 and TUJ1 expression in cell couplets 20 hours post plating.

(I) Division type (% total number of couplets identified per embryo) in couplets from control, Foxp1^{ON} and Foxp1^{OFF} cortices.

(J) Division type in couplets involving at least one RG (% total RG divisions) from control, Foxp1^{ON} and Foxp1^{OFF} embryos. Mean ± SEM from 2 litters per genotype. Between 200-400 couplets per embryo were counted. N = 11 control embryos, 9 Foxp1^{ON} embryos and 4 Foxp1^{OFF} embryos (I, J). Significance was determined by One-way ANOVA with post-hoc multiple comparison test, *p <0.05; **p <0.005; ***p <0.001. RG, radial glia; IP, intermediate progenitor; N, neuron. Scale bars; 100 μm E, F; 5 μm G, H.
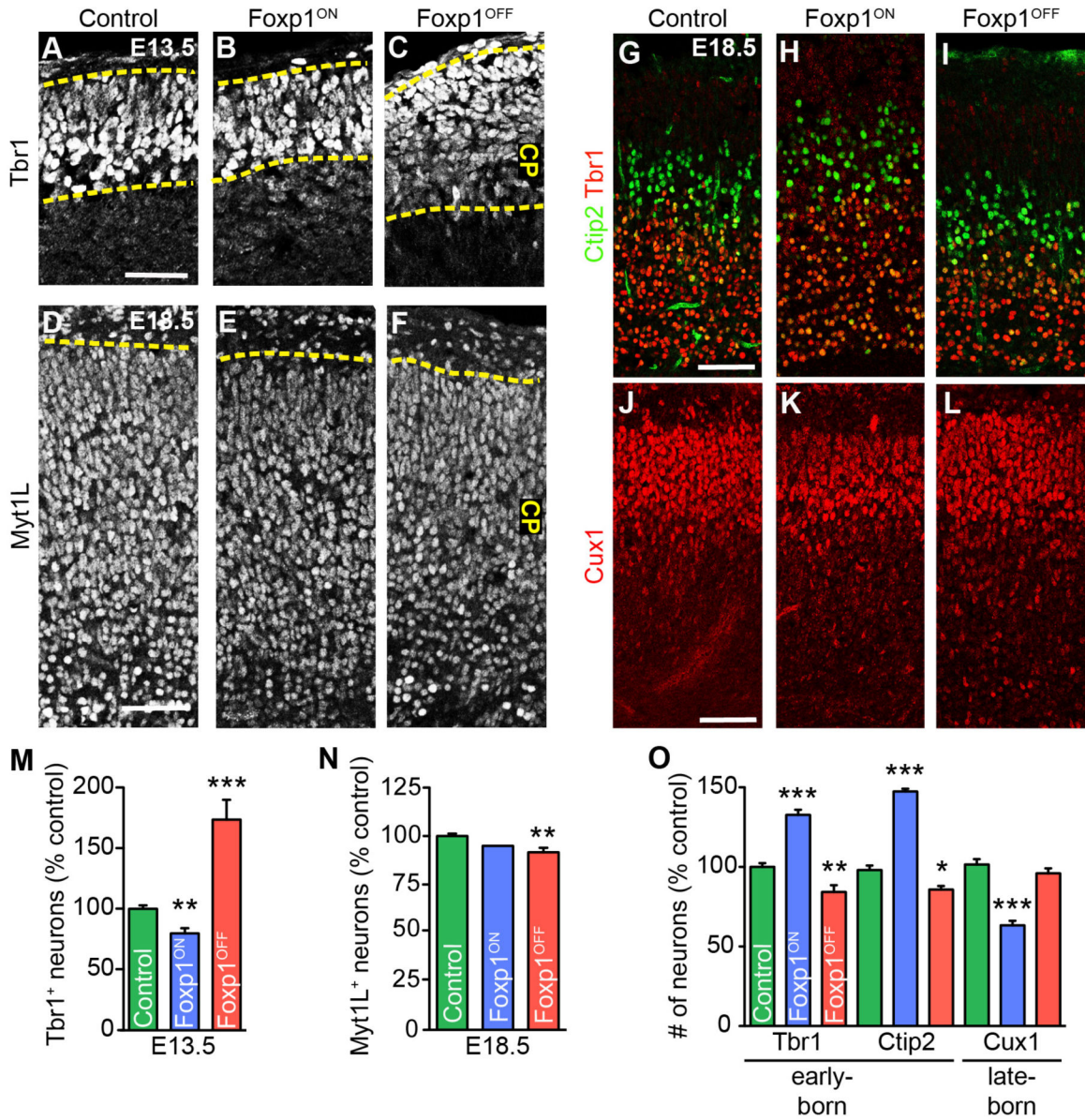
Figure 4. Foxp1 promotes aRG maintenance at the expense of neurogenesis

(A-C) Tbr1 expression in control, Foxp1[ON] and Foxp1[OFF] embryos at E13.5.

(D-F) Myt1l expression in control, Foxp1[ON] and Foxp1[OFF] embryos at E18.5. Dashed yellow lines mark CP.

(G-I) Ctip2 and Tbr1 expression in the CP at E18.5 in control, Foxp1[ON] and Foxp1[OFF] embryos.

(J-L) Cux1 expression in the CP at E18.5 in control, Foxp1[ON] and Foxp1[OFF] embryos.

(M) Number of Tbr1^{+} neurons (% control) at E13.5 in control, Foxp1[ON] and Foxp1[OFF] embryos. Mean number $\pm$ SEM from at least 3 sections per embryo. N= 3 litters per genotype; 12 control embryos, 9 Foxp1[ON] embryos, 5 Foxp1[OFF] embryos.

(N) Number of Myt1l^{+} neurons (% control) at E18.5 in control, Foxp1[ON] and Foxp1[OFF] embryos. Mean number ± SEM from at least 3 sections per embryo. N= 2 litters per genotype; 10 control embryos, 3 Foxp1[ON] embryos, 3 Foxp1[OFF] embryos.

(O) Number of early and late born neurons in E18.5 control, Foxp1[ON] and Foxp1[OFF] conditions (% control). Mean ± SEM from at 4-5 sections per embryo. N = 3 litters per genotype; 14 control, 8 Foxp1[ON] embryos, 6 Foxp1[OFF] embryos. Significance was determined using One-way ANOVA with post-hoc multiple comparison test, *p <0.05; **p <0.005; ***p <0.001; ****p <0.0001. Scale bars; 50 μm. See also Figures S3 and S4.
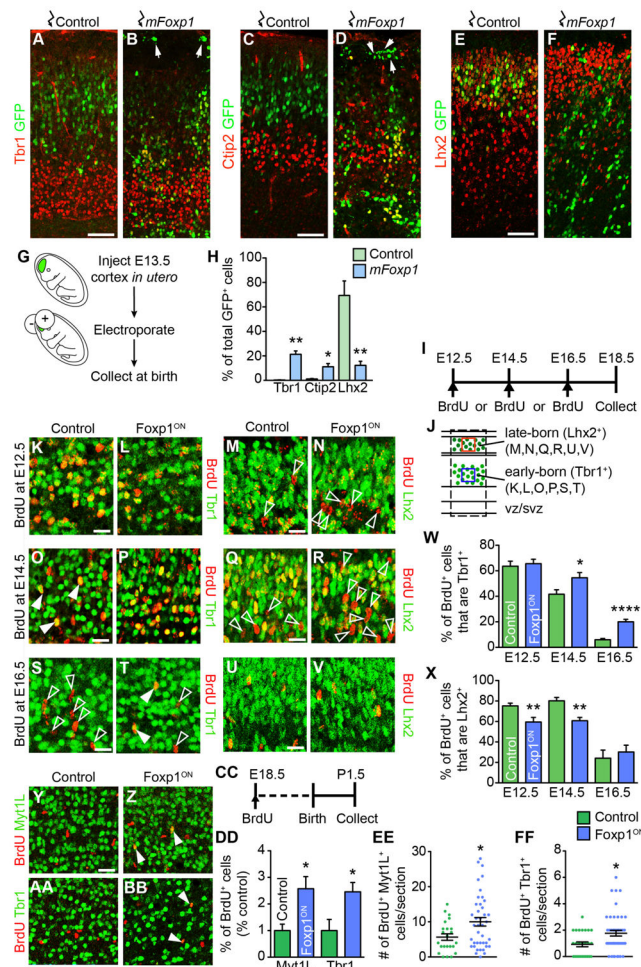
Figure 5. Sustained Foxp1 expression extends the window of early neurogenesis into later stages of development.

(A-F) Tbr1, Ctip2, and Lhx2 expression in P0.5 cortices electroporated at E13.5 with IRES-GFP control or mFoxp1-IRES-GFP expression plasmids.

(G) Schematic of electroporation protocol.

(H) Percentage of GFP^{+} cells expressing Tbr1, Ctip2 and Lhx2 in embryos electroporated with IRES-GFP control or mFoxp1-IRES-GFP expression plasmids. Mean percentage ± SEM from 4-5 sections per pup. N= 2 litters, 4 pups per condition.

(I) Schematic of experimental design.

(J) Tbr1 and Lhx2 were used to identify early born and late born neurons respectively. Red and blue boxes within denote distinct areas of the cortical plate that are represented in the images below.

(K-N) Immunostaining for BrdU and Tbr1 and Lhx2 in control and Foxp1[ON] embryos pulse labeled with BrdU at E12.5. Clear arrowheads denote BrdU only cells.

(O-R) Immunostaining for BrdU and Tbr1 and Lhx2 in control and Foxp1[ON] embryos pulse labeled with BrdU at E14.5. Filled arrowheads denote BrdU[+]/Tbr1^{+} cells.

(S-V) Immunostaining for BrdU and Tbr1 and Lhx2 in control and Foxp1[ON] embryos pulse labeled with BrdU at E16.5.

(W) Percentage of BrdU-labeled cells expressing Tbr1 after injection at E12.5, E14.5 or E16.5.

(X) Percentage of BrdU-labeled cells expressing Lhx2 after injection at E12.5, E14.5 or E16.5. Mean ± SEM from 4 sections from each embryo. N= 2 litters per timepoint, 4-5 control embryos per timepoint, 5 Foxp1^{ON} embryos per timepoint (W and X).

(Y-Z) Immunostaining for BrdU and Myt1l at P1.5 in control and Foxp1^{ON} pups injected with BrdU at E18.5. Arrowheads indicate BrdU$^+$Myt1l$^+$ cells.

(AA-BB) Immunostaining for BrdU and Tbr1 at P1.5 in control and Foxp1^{ON} pups injected with BrdU at E18.5. Arrowheads indicate BrdU$^+$Tbr1$^+$ cells.

(CC) Schematic of experimental design.

(DD) Percentage of BrdU$^+$ cells (% control) expressing Myt1l and Tbr1 in control and Foxp1^{ON} pups. Mean ± SEM from at least 3 sections per pup. N= 2 litters, 4 control pups and 7 Foxp1^{ON} pups. Significance was determined using Mann Whitney test, *p <0.05.

(EE-FF) Number of BrdU$^+$ Myt1l$^+$ and BrdU$^+$ Tbr1$^+$ cells per section in control and Foxp1^{ON} conditions. Mean ± SEM from ~35 sections per genotype from 4 control pups and 7 Foxp1^{ON} pups from 2 litters. Significance was determined using a Student's t-test (unless otherwise stated). *p <0.05; **p <0.005; ***p <0.001; ****p <0.0001.

Scale bars; 50 μm A-F, 20 μm K-BB. See also Figures S4 and S5.
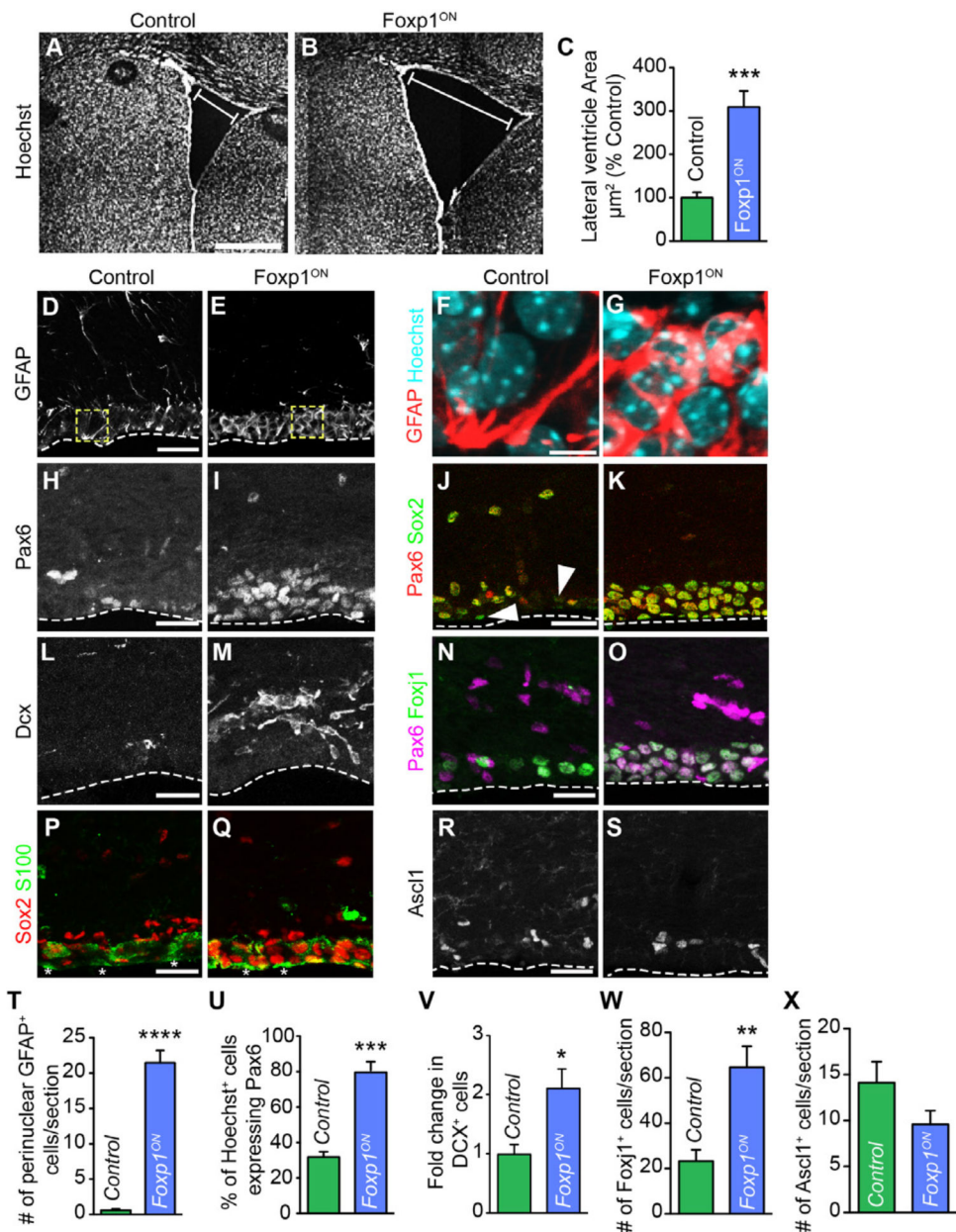
Figure 6. Foxp1 can sustain an aRG-like population into adulthood.

(A-B) Analysis of lateral ventricle size in 6-week-old control and Foxp1^{ON} animals.

(C) Area of lateral ventricle (% control) in control and Foxp1^{ON} animals at 6 weeks old.

(D-E) GFAP expression in the dorsal lateral ventricle in control and Foxp1^{ON} animals. Dashed yellow boxes mark area in F-G.

(F-G) GFAP localization in the SVZ region with nuclei labeled with Hoechst in control and Foxp1^{ON} animals.

(H-I) Pax6 expression in control and Foxp1^{ON} animals.

(J-K) Pax6 and Sox2 expression in control and Foxp1^{ON} animals. Arrowheads denote Sox2^{+} Pax6^{-} cells.

(L-M) Dcx expression in control and Foxp1^{ON} animals.

(N-O) Foxj1 and Pax6 expression in control and Foxp1[ON] animals.

(P-Q) Sox2 and S100 expression in control and Foxp1[ON] animals.

(R-S) Ascl1 expression in control and Foxp1[ON] animals.

(T) Number of cells with perinuclear GFAP staining per section within the lining of the lateral ventricle in 6-week control and Foxp1[ON] animals.

(U) Percentage of nuclei lining the lateral ventricles expressing Pax6 in 6-week control and Foxp1[ON] animals.

(V) Fold change in number of DCX^{+} cells in week 6 control and Foxp1[ON] animals.

(W) Number of Foxj1^{+} cells per section in 6-week control and Foxp1[ON] animals.

(X) Number of Ascl1^{+} cells per section in 6-week control and Foxp1[ON] animals.

Mean ± SEM from 3-4 sections per animal. N= 3 litters, 5 control animals, 3 Foxp1[ON] animals (C, T-X). Significance was determined using the Student's t-test. *p <0.05; **p <0.005; ***p <0.001; ****p <0.0001. Scale bars; 500µm A-B, 50 µm D, E, H-S, 5 µm F-G. See also Figure S6.
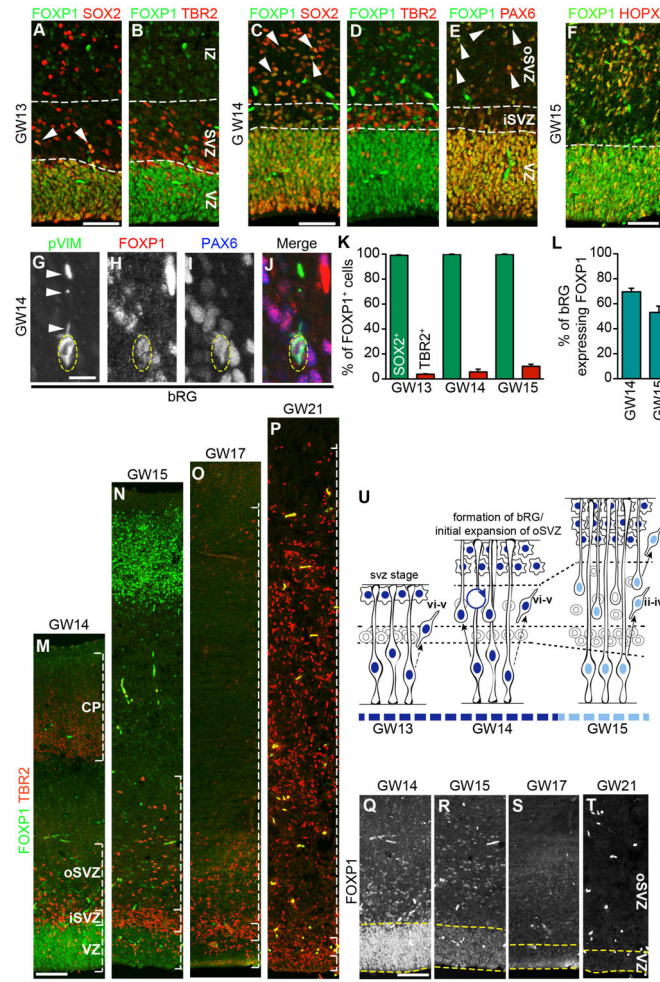
Figure 7. Foxp1 is expressed by both aRG and bRG in the developing human cortex

(A-B) FOXP1, SOX2 and TBR2 expression in the VZ and SVZ in the GW13 cortex. Dashed white lines mark VZ and SVZ.

(C-E) FOXP1, SOX2, TBR2 and PAX6 at GW14. Arrowheads indicate double positive cells.

(F) FOXP1 and HOPX expression at GW15.

(G-J) pVIM, FOXP1 and PAX6 expression in the oSVZ at GW14. Yellow oval marks the nucleus in each channel. White arrows indicate pVIM staining in basal process

(K) Percentage of FOXP1$^+$ cells expressing either SOX2 or TBR2 at GW13, 14 and 15.

(L) Percentage of bRG expressing FOXP1 at GW14 and 15.

(M-P) FOXP1 expression levels in the VZ/oSVZ from GW14-21. TBR2 immunostaining demonstrates the expansion of the iSVZ/oSVZ.

(Q-T) FOXP1 expression between GW14-21 in the VZ/oSVZ (single channel images from M-P).

(U) Schematic to demonstrate high expression of FOXP1 in aRG and bRG during early human corticogenesis at the onset of bRG generation/oSVZ formation. From GW15 onwards FOXP1 levels decrease.
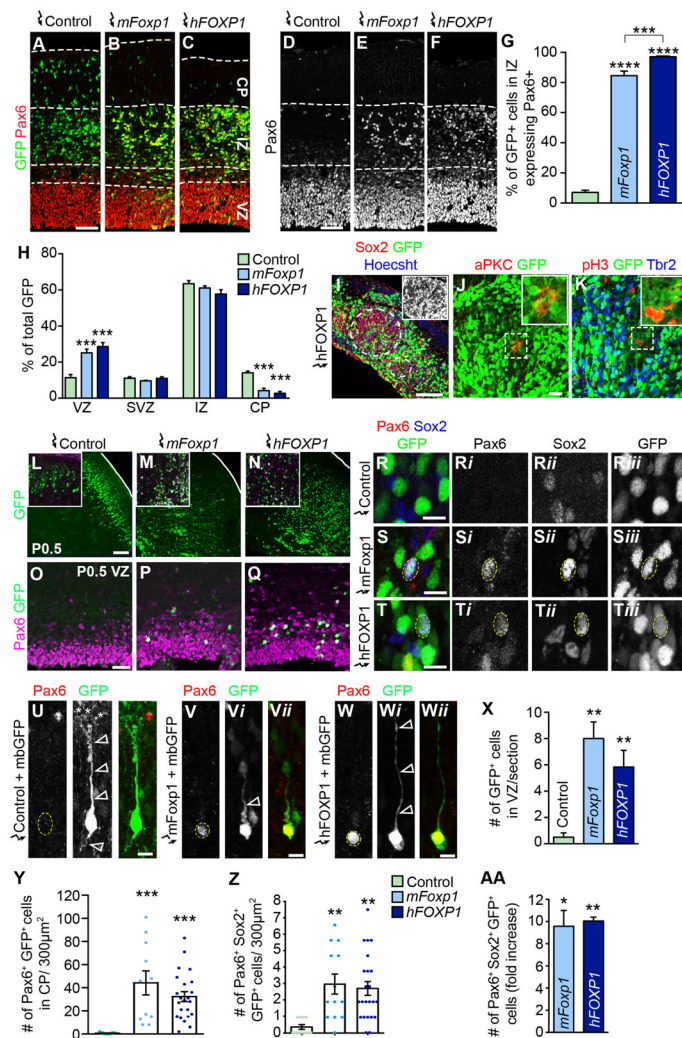
VZ, ventricular zone; SVZ, subventricular zone; IZ, intermediate zone; iSVZ, inner subventricular zone; oSVZ, outer subventricular zone; bRG, basal radial glia; CP, cortical plate. Scale bars; 50 μm A-F, 10 μm G-J, and 100 μm M-T.

Figure 8. Acute misexpression of Foxp1 during mid-neurogenesis preserves progenitor characteristics.

(A-C) GFP and Pax6 expression in cortices electroporated with control-IRES-GFP, mFoxp1 and hFOXP1 plasmids at E13.5 and collected 2 days post-electroporation (E15.5). White dashed lines demarcate boundaries of the VZ, SVZ, IZ and CP.

(D-F) Pax6 expression alone from A-C.

(G) Percentage of GFP^{+} cells in the IZ expressing Pax6^{+} in control, mFoxp1 and hFOXP1-electroporated cortices.

(H) Spatial distribution of GFP^{+} cells in cortices electroporated at E13.5 and collected at E15.5. Mean ± SEM from 4-5 sections per embryo. N= 2 litters, 10 controls, 5 mFoxp1, 8 hFOXP1 (G and H).

(I-K) Sox2, aPKC, pH3 and Tbr2 expression in neural rosettes in cortices 2 days after electroporation with hFOXP1. White circles demarcate neural rosettes. Dashed box indicates inset in J. Arrowheads mark apical pH3^{+} cells in the rosettes. Inset in I shows GFP only. Insets in J and K high magnification image of center of rosette demonstrating broad GFP expression within the ectopic rosettes.

(L-N) Distribution of GFP$^+$ cells in cortices electroporated at E13.5 with control, mFoxp1, or hFOXP1 expression plasmids and collected at P0.5. Insets show immunostaining for Pax6 (magenta) and GFP.

(O-Q) Pax6 expression in the VZ of electroporated P0.5 cortices.

(R-T) Pax6/Sox2 double positive cells in P0.5 cortices electroporated with control or Foxp1 expression constructs.

(U-W) Analysis of mbGFP and Pax6 expression in unipolar abventricular cells resembling bRG in P0.5 cortices co-electroporated with control GFP, mFoxp1 or hFoxp1 and mbGFP. Cell soma outlined by yellow dashed lines. Processes indicated by white arrowheads. Some cells transfected with the control plasmids lacked Pax6 staining and displayed processes with complex endings resembling dendrites (asterisks). By contrast, cells expressing either mFoxp1 or hFOXP1 expressed Pax6 and exhibited single thin processes.

(X) Number of GFP$^+$ cells within the P0.5 VZ after electroporation with control, mFoxp1, or hFOXP1 plasmids.

(Y) Number of GFP$^+$ Pax6$^+$ cells in the cortical plate (per 300 μm^2) in control and Foxp1-electroporated P0.5 cortices.

(Z) Number of Pax6/Sox2/GFP triple positive cells (per 300 μm^2) in control and Foxp1-electroporated P0.5 cortices.

(AA) Fold increase (over control) in number of Pax6/Sox2/GFP triple positive cells in cortices electroporated with mouse and human Foxp1. Mean ± SEM from 5 sections per pup. N= 2 litters, 4 pups per condition (X-AA). Significance determined using One-way ANOVA with post-hoc multiple comparisons test. *p <0.05; **p <0.005; ***p <0.001; ****p <0.0001. Scale bars; 50 μm A-F, 100 μm L-N, 50 μm O-Q, 10 μm R-T, U, V, W. VZ, ventricular zone; SVZ, subventricular zone; IZ, intermediate zone; CP, cortical plate. See also Figure S8.

KEY RESOURCES TABLE

REAGENT or RESOURCE	SOURCE	IDENTIFIER
Antibodies		
ASCL1	BD Pharmingen	Cat# 556604; RRID AB_396479
BLBP	Chemicon	Cat# AB9558; RRID AB_2314014
BrdU (MAS250p)	Accurate Chemical	Cat# OBT0030; RRID AB_2341179
CALRETININ	Millipore	Cat# AB5054; RRID AB_2068506
CLEAVED CASPASE 3	Cell Signaling	Cat# 9661S; RRID AB_2341188
CTIP2 (BC11B)	Abcam	Cat# AB18465; RRID AB_2064130
CUX1 (M222)	Santa Cruz	Cat# SC13024; RRID AB_2261231
DCX	Millipore	Cat# AB2253; RRID AB_1586992
FOXP1	Novitch Lab (Rousso et al., 2008)	RRID AB_2811723
FOXP2	Abcam	Cat# AB16046; RRID AB_2107107
FOXP4	Millipore	Cat# ABE74; RRID AB_10617521
GFAP	BD Pharmingen	Cat# 556330; RRID AB_396368
GFP	Aves Lab Inc.	Cat# GFP-1020; RRID AB_10000240
GFP	ABD Serotec	Cat# 4745-1051; RRID AB_619712
Phosphorylated HISTONE H3	Cell Signaling	Cat# 9701S; RRID AB_331535
HOPX	Sigma Aldrich	Cat# HPA030180; RRID AB_10603770
LHX2	Santa Cruz	Cat# Sc-19344; RRID AB_2135660
MYT1L	Dr. Marius Wernig, Stanford University (Mall et al., 2017)	N/A
PAX6	MBL International	Cat# PD022; RRID AB_1520876
Atypical PKC	Santa Cruz	Cat# SC216; RRID AB_2300359
S100	Sigma Aldrich	Cat# S2644; RRID AB_477501
SOX2 (Y-17)	Santa Cruz	Cat# SC17320; RRID AB_2286684
TBR1	Abcam	Cat# Ab31940; RRID AB_2200219
TBR2	Millipore	Cat# Ab15894; RRID AB_10615604
TUJ1	Covance	Cat# MMS-435p; RRID AB_2313773
Phosphorylated VIMENTIN	MBL International	Cat# D076-3; RRID AB_592963
Bacterial and Virus Strains		
N/A		
Biological Samples		
Human fetal brain tissue	Novogenix Laboratories	N/A
Human fetal brain tissue	University of Tübingen	N/A
Experimental Models: Organisms/Strains		

REAGENT or RESOURCE	SOURCE	IDENTIFIER
Mouse: Foxp1A transgenic	Dr. Hui Hu, University of Alabama (Wang et al., 2014)	MGI:5607369
Mouse: Foxp1$^{flox/flox}$	Dr. Haley Tucker, University of Texas (Feng et al., 2010)	RRID:MGI:4421659
Mouse: Emx1$^{Cre(Tg)}$	RIKEN BioResource Center (Iwasato et al., 2004)	MGI:3033255
Mouse: Emx1$^{Cre(KI)}$	The Jackson Laboratory stock #005628 (Gorski et al., 2002)	RRID:IMSR_JAX:005628
Mouse: Nex1^{Cre}	Drs. Sanda Goebbels and Klaus Nave, Max Planck Institute of Experimental Medicine (Goebbels et al., 2006)	MGI:3695526
Oligonucleotides		
In situ probe for Foxp1 3'UTR: Forward primer tcagcatcaggaaacaca	This paper	N/A
In situ probe for Foxp1 3'UTR: Reverse primer gagattaaccctcactaaagggagtct	This paper	N/A
Recombinant DNA		
pCIG	Dr. Andrew McMahon (Megason and McMahon, 2002)	N/A
pCIG-human Foxp1	Novitch lab (Adams et al., 2015)	N/A
pCIG-mouse Foxp1	Novitch Lab (Rousso et al., 2008)	N/A
Software and Algorithms		
Zen Blue	Carl Zeiss Microscopy	Zen 2.3; RRID:SCR_013672
Adobe Photoshop	Adobe Systems	CS5, CC2017-2019; RRID:SCR_014199
Adobe Illustrator	Adobe Systems	CS5, CC2017-2019; RRID:SCR_010279
Primer3 Plus	Wageningen University and Research Centre	http://primer3plus.com; RRID:SCR_003081
(Fiji is just) ImageJ	Max Planck Institute of Molecular Cell Biology and Genetics	Version 2 2016: RRID:SCR_002285
Graphpad Prism	Graphpad	Versions 6, 7, or 8; RRID:SCR_002798